Proj. #157A

24569

Modeling of thermoelastic generation of ultrasound in oil upon water

Task 2 - FINAL REPORT

Marc Choquet and Jean-Pierre Monchalin
Industrial Material Institute
National Research Concil of Canada
75 de Mortagne Blvd, Boucherville (Québec)
J4B-6Y4, Canada

P. #157

29 November, 1990

Modeling of thermoelastic generation of ultrasound in oil upon water

Task 2 - FINAL REPORT

Marc Choquet and Jean-Pierre Monchalin
Industrial Material Institute
National Research Concil of Canada
75 de Mortagne Blvd, Boucherville (Québec)
J4B-6Y4, Canada

29 November, 1990

1 INTRODUCTION

In a previous investigation[1], we have demonstrated the feasibility of using laser-ultrasonics for measuring the thickness of an oil layer floating on top of water. The purpose of this study was to establish the possibility of using laser-ultrasonics for remote sensing of an oil spill from an airplane. We have concluded that such application seems feasible but that further work is needed, in particular in order to establish the optimum conditions of measurement. In this report, we present a computer model we have developed for simulation of the laser-ultrasonic interaction in this case, and which allows us to study the influence of the various measurement parameters.

Laser-ultrasonics, as used in this application, is based on the thermoelastic generation of ultrasound following a local heating of the sample by a pulsed optical beam[2]. As the sample thermally expands, an acoustic wave is then generated. The surface motion of the sample is detected by a probe beam which is frequency shifted by the Doppler effect upon reflection by the surface. This frequency shift of the probe beam is then detected by a Fabry-Pérot interferometer. Since we have an oil layer on top of water, reflection of the laser generated acoustic pulse is encountered at the layer-water interface, giving an acoustic echo. By measuring the time interval between the echo and the front surface deformation and knowing the acoustic velocity, the thickness of the layer can then be determined.

The model we have developed can be subdivided into two parts. In the first part, we calculate the thermoelastic displacement of the surface following optical absorption of the laser pulse with a given time variation. In the second part, we calculate the signal at the output of the Fabry-Pérot which is illuminated by the probe beam reflected by the sample surface. Using this model, we are able to assess the effect of Fabry-Pérot finesse and laser energy on the sensitivity and accuracy of the measurement.

2 MODELING THE THERMOELASTIC DISPLACEMENT OF A TWO LAYER SYSTEM

2.1 Conditions of the model

In this section, we calculate for a two media system, the displacement produced by the optical absorption of a laser pulse, as function of time and

depth. The first medium has a finite thickness L, whereas the thickness of the second medium (substrate) is sufficiently large so as to be considered as infinite. We also assume that the generation of the acoustic wave is in the thermoelastic regime. This means that the signal is created only by the absorption of the optical beam. Depth penetration of the beam and of the resulting heat source follows an exponential decay (Beer's law). The acoustic wave is generated by the thermal expansion which take place in the heated medium. The laser pulse energy is assumed to be sufficiently low, so that no ablation or evaporation of the sample can be observed.

Since our time scale for the simulation is small, generally of the order of 10 μsec, thermal diffusion can be neglected. The temperature variation at a given location is then only dependent upon the amount of optical energy deposited at this location. We will also assume that no thermal energy is generated by the propagation of the acoustic wave. This means essentially that we are neglecting thermal loss during ultrasonic propagation, which is an excellent approximation.

Modeling will be limited to one-dimension and we will assume uniform laser light distribution at the sample surface. This also means that we neglect any shear wave motion in the sample. Notice that this condition is generally valid for low viscosity liquid samples. It should be noted that neglecting viscosity as well as thermal loss means that there is no attenuation of the acoustic wave.

Concerning the boundary conditions, the top surface is assumed to be free of any stress. We do not consider any surface or capillary wave. We also assume that the interface between the layer and the water substrate is ideal, which means that there is continuity of the displacement and of the normal stress. It should be noted that since we neglect heat diffusion, there is discontinuity of temperature at the interface.

2.2 Solution of the thermal equations

Since thermal diffusion is neglected, the temperature is proportional to the total amount of energy deposited at a given depth x by optical absorption. The temperature is given by the Fourier equation for each medium, with their thermal diffusivity equal to zero. This equation is then for the layer, i.e. $x \in [0,L]$,

$$\rho_1 C_1 \frac{\partial T(x,t)}{\partial t} = \alpha_1 e^{-\alpha_1 x} \Phi_0 F(t) \quad (1)$$

and for the substrate, i.e. $x \in [L, \infty[$,

$$\rho_2 C_2 \frac{\partial T(x,t)}{\partial t} = \alpha_2 e^{-\alpha_1 L} e^{-\alpha_2 (x-L)} \Phi_0 F(t) \quad (2)$$

where T(x,t) is the temperature variation at position x and time t (°K), ρ_i is the media density (kg/m^3), C_i is the specific heat (J kg/°K), Φ_0 is the peak power density at the surface (W/m^2), α_i is the optical absorption coefficient (m^{-1}), and F(t) is the normalized laser pulse shape. These equations can be simply solve by integrating both sides with respect to time and by specifying that:

$$T(x,t=0) = 0 \quad (3)$$

Then, for $x \in [0,L]$,

$$T(x,t) = \Phi_0 \frac{\alpha_1}{\rho_1 C_1} e^{-\alpha_1 x} \int_0^t F(\xi)\, d\xi \quad (4)$$

and for $x \in [L,\infty[$,

$$T(x,t) = \Phi_0 \frac{\alpha_2}{\rho_2 C_2} e^{-\alpha_1 L} e^{-\alpha_2 (z-L)} \int_0^t F(\xi)\, d\xi \quad (5)$$

We immediately notice that the temperature variation at a given point is proportional to the time integral of the laser pulse, i.e. to the total amount of energy absorbed, as expected.

2.3 Solution of the acoustic equations

In our model, the acoustic wave is generated by the thermal expansion of the sample resulting from the local temperature elevation caused by absorption of the laser pulse. For each medium, acoustic generation and propagation is described by the Navier-Stokes displacement equation, where convective effects have been neglected. Therefore, the displacement u(x,t) is given by

$$\rho_i \frac{\partial^2 u(x,t)}{\partial t^2} = (\lambda_i + 2\mu_i) \frac{\partial^2 u(x,t)}{\partial x^2} - (3\lambda_i + 2\mu_i) \alpha_{T_i} \frac{\partial T(x,t)}{\partial x} \quad (6)$$

and the stress $\sigma(x,t)$ is given by

$$\sigma(x,t) = (\lambda_i + 2\mu_i)\frac{\partial u(x,t)}{\partial x} - (3\lambda_i + 2\mu_i)\alpha_{T_i} T(x,t) \qquad (7)$$

where λ_i and μ_i are the Lamé constants (N/m^2), α_{T_i} is the thermal expansion coefficient ($°K^{-1}$), with i=1 for oil and i=2 for water. Notice that for low viscosity liquids, the Lamé constant μ is zero.

Concerning the boundary conditions, we note first that the surface of the sample is free to move. Therefore, there is no stress at the front surface (x=0), i.e.

$$\sigma(x=0,t) = 0 \qquad (8)$$

Secondly, the interface between the two layers is assumed to be ideal. This means that there are continuity of displacement and continuity of stress through the interface, i.e.

$$\begin{cases} u(L^+,t) = u(L^-,t) \\ \sigma(L^+,t) = \sigma(L^-,t) \end{cases} \qquad (9)$$

Applying Laplace transform to equation 6, we immediately identify that the solution of the displacement has the form

$$U(x,s) = \begin{cases} \left[U_1(s)\, e^{-k_1(s)(L-x)} + U_2(s)\, e^{-k_1(s)\,x} + \psi_1(s)\, e^{-\alpha_1 x}\right] F(s) & \text{for } x \in [0,L] \\ \left[U_3(s)\, e^{-k_2(s)\,x} + \psi_2(s)\, e^{-\alpha_1 L}\, e^{-\alpha_2(x-L)}\right] F(s) & \text{for } x \in [L,\infty] \end{cases} \qquad (10)$$

where U(x,s) is the Laplace transform of u(x,t), F(s) is the Laplace transform of the pulse shape F(t), $U_1(s)$, $U_2(s)$ and $U_3(s)$ are functions of s given by the boundary conditions, and the $\psi_i(s)$ functions are given by

$$\psi_i(s) = \frac{\alpha_i^2 (3\lambda_i + 2\mu_i)\alpha_{T_i}}{s\,\rho_i\, C_i \left[\rho_i s^2 - (\lambda_i + 2\mu_i)\alpha_i^2\right]} \Phi_0 \qquad (11)$$

with i=1 for oil and i=2 for water.

With the use of Laplace transform, the boundary conditions can be written as a matrix equation. Inversion of this matrix leads to the expression of $U_1(s)$, $U_2(s)$ and $U_3(s)$. After some calculations, the final expressions are

$$U_1(s) = -\frac{(1-z_r)\, r_1\, \psi_1\, e^{-k_1 L} - [(r_1 - z_r)\psi_1 - z_r(r_2 - 1)\psi_2]\, e^{-\alpha_1 L}}{(1 + z_r) - (1 - z_r)\, e^{-2k_1 L}} \tag{12}$$

$$U_2(s) = -\frac{(1+z_r)\, r_1\, \psi_1 - [(r_1 - z_r)\psi_1 - z_r(r_2 - 1)\psi_2]\, e^{-(\alpha_1 + k_1)L}}{(1 + z_r) - (1 - z_r)\, e^{-2k_1 L}} \tag{13}$$

$$U_3(s) = \frac{-2r_1\, \psi_1\, e^{-k_1 L} + [(1 + r_1) - (1 - r_1)\, e^{-2k_1 L}]\, \psi_1\, e^{-\alpha_1 L}}{(1 + z_r) - (1 - z_r)\, e^{-2k_1 L}} + \frac{[(1 + z_r r_2) - (1 - z_r r_2)\, e^{-2k_1 L}]\, \psi_2\, e^{-\alpha_1 L}}{(1 + z_r) - (1 - z_r)\, e^{-2k_1 L}} \tag{14}$$

with

$$z_r = \sqrt{\frac{\rho_2(\lambda_2 + 2\mu_2)}{\rho_1(\lambda_1 + 2\mu_1)}} \tag{15}$$

$$r_i(s) = \frac{s}{\alpha_i}\sqrt{\frac{\rho_i}{\lambda_i + 2\mu_i}} \tag{16}$$

and

$$k_i(s) = s\sqrt{\frac{\rho_i}{\lambda_i + 2\mu_i}} \tag{17}$$

These expressions are too complex for calculating the inverse transform of U(x,s). This transform can, however, be derived by numerical calculation. It should be noted that using of a numerical approach to the Laplace transform inversion means that we can use any pulse shape for the heating laser.

With this approach, the thermoelastic displacement of the surface of a layer of oil on top of water can be calculated. The values of the parameters used are indicated in table 1. Figure 1 show the surface displacement of a 1 mm thick oil layer on a water substrate using a normalized pulse shape of the form

$$F(t) = \frac{t}{\tau} e^{\left(1 - \frac{t}{\tau}\right)} \tag{18}$$

The rise time τ was taken to be 100 nsec and the pulse energy was assumed to be 10 mJ uniformly distributed over a spot of 6 mm in diameter. The displacement

shows a large step-like rise which resembles the integration of the pulse shape. We also observe a series of echoes arriving at periodic time resulting from reflections by the interface. It should be noted that the diminishing amplitude of the echoes is not related to acoustic attenuation, since our model does not consider viscosity nor thermal losses. This attenuation results from the transmission of the acoustic wave through the oil-water interface. Since the acoustic impedances of oil and water have values close to each other, the reflection coefficient is low (≈0.18). Therefore, only a small portion of the acoustic wave incident onto the interface is reflected back to the surface.

3 CALCULATION OF THE SIGNAL FROM THE FABRY-PÉROT

In laser-ultrasonics, the displacement of the sample surface is monitored by a probe beam reflected by the surface[2]. The movement of the surface produces a phase shift of the probe beam which is then measured by the Fabry-Pérot interferometer. The light field at the output of a Fabry-Pérot (FP) is composed of the sum of many retarded waves following multiple reflections within the cavity of the interferometer. Given a light field E(t), reflected by a surface at some distance D, incident onto a planar FP, the transmitted field by the FP is given by

$$S(t) = \sum_{n=0}^{\infty} t'_1 (r_1 r_2)^n t_2 E(t-t_0-2n\tau) \qquad (19)$$

where t'_1, t_2, r_1 and r_2 are the complex transmission and reflection coefficients of the mirrors of the FP, t_0 is the propagation time between the static surface and the output mirror of the FP, and 2τ is the delay introduce by the FP, i.e. the transmission time in the FP cavity (τ=e/c where e is the length of the cavity and c is the speed of light). If the surface is displaced by u(t) in the direction of the FP, then the light wave will arrive at time t_0-2u(t)/c instead of t_0. The light field transmitted by the FP is then

$$S(t) = \sum_{n=0}^{\infty} t'_1 (r_1 r_2)^n t_2 E\left(t - t_0 - \frac{2u(0,t-t_0-2n\tau)}{c} - 2n\tau\right) \qquad (20)$$

In the same same way, we can calculate the reflected light field and the effect of the surface displacement upon it.

Using u(0,t) derived with the model of the preceding section, we are then able to calculated the signal given by the FP resulting from the thermoelastic displacement of the two-layers system. Notice that the term in the series decreases rapidly as $(r1r2)^n$ (since $|r1r2|<1$). We can therefore limit the series to a value N such that the contribution of all terms for n>N are negligible. This allows to accelerate the numerical calculation of S(t).

The response of the FP is therefore directly calculated by summing, in complex notation, the retarded waves. The transmitted or reflected wave is received by an optical detector which is sensitive to the intensity of the signal. The measured signal I(t) is then given by

$$I(t) = |S(t)|^2 \tag{21}$$

These equations are valid for a planar FP. In order, to increase the light gathering power of the receiver, the laser-ultrasonics system uses instead a confocal FP. The calculation of the transmitted and reflected waves is similar to that of the planar FP except that we must consider four output beams (two in reflection and two in transmission) instead of two. As with the planar FP, the series can be limited to a finite number of terms N.

In order to accelerate computation, the surface displacement and the signals from the FP are sampled in unit of $\tau=e/c$. If the time origin is set such that $t_0=0$, then equation 20 can be rewritten as

$$S(i\tau) = \sum_{n=0}^{\infty} t_1' (r_1 r_2)^n t_2 E\left((i-2n)\tau - \frac{2u(0,(i-2n)\tau)}{c}\right) \tag{22}$$

While this approach accelerates computation, it fixes the sampling rate to τ. Figure 2 shows the signal from a confocal Fabry-Pérot, operating in transmission, produced by the surface displacement of figure 1. The confocal Fabry-Pérot has a cavity length of 1 m, reflection coefficient for both mirrors of 0.85% and the probe beam wavelength is 1.06 µm. We notice that the initial surface displacement produces a large mono-polar pulse. The echoes can be clearly observed as bipolar pulses at regular time intervals.

4 DESCRIPTION OF THE PC-BASED COMPUTER PROGRAM

Having determined the theoretical expressions for the surface displacement and for the response of the confocal Fabry-Pérot, we have implemented them in a program for personal computer. This program is meant to be user-friendly and to rely to a large extent on graphic presentation. The calculation of the simulation is made in three steps. First, the program sets the pulse shape of the heating laser. As we will see, this shape can be either a theoretical expression or the actually sampled pulse shape data. Secondly, the surface displacement of the sample resulting from thermoelastic deformation is computed using numerical forward and inverse Laplace transform. Finally, the response of the confocal Fabry-Pérot receiver to this surface displacement is calculated by direct summation in complex notation of the multiple retarded waves.

In the section below, we describe first the different functions of the program following the order of their presentation in the main menu. We then give an example of the use of the program.

4.1 Overview of commands

When the program is initially started, the list of the available functions is displayed on the screen (see figure 3). To select a particular function, the user moves the cursor (box) with the UP and DOWN key to the appropriate position, and presses ENTER to engage the function. To exit from any function, the ESC key should be pressed. This, depending on the selected function, will start the computation of the selected option and return the user to the main menu.

4.1.1 Edit a sample file

This function permits the user to enter the different parameters needed in the calculation of the thermoelastic displacement of the sample. To set a value, move the cursor with the UP or DOWN keys to the appropriate parameter, then press ENTER. The box is now empty and the user can enter the new value in scientific format (i.e. 1.203e+6). Pressing ENTER again will set the new value. In exiting from this function, by pressing the ESC key, the parameters values are stored in a file name *name_of_sample*.PRM. The values of these files can be

recalled by setting the NAME OF SAMPLE variable to the name of the file (for example OIL).

It should be noticed that although the shear velocity is required, the model does not compute the shear wave (one-dimensional model). The shear velocity is only used to determine the Lamé constants of the sample. The shear velocity is used as input parameter since it is usually easier to get this value in the literature than the Lamé constants.

4.1.2 Compute the pulse shape of the heating laser

This is the first step of the simulation. The pulse shape is computed following the parameters set with the SET SIMULATION PARAMETERS function. The default shape is a pulse of the form given by equation 18 with a rise time τ=100 nsec, a pulse energy of 10 mJ, and a spot radius of 3 mm. After engaging this procedure, the program plots automatically the pulse shape as a function of time.

4.1.3 Compute the thermoelastic displacement of a two layer system

This is the second step of the simulation. As for the pulse shape, the parameters of the calculation are set with the SET SIMULATION PARAMETERS function. In the default mode, the program computes the thermoelastic surface displacement of a 1 mm oil layer on water resulting from the absorption of the laser pulse previously computed. After engaging this procedure, the program plots automatically the displacement as a function of time.

4.1.4 Compute the response of a Fabry-Pérot to the surface displacement

Finally, in this last step of the simulation, the program computes the response of the FP to the previously computed displacement. It should be noted that this calculation can be quite long depending upon the values of the reflection coefficients of the mirrors. As for the pulse shape and the thermoelastic displacement, the parameters of the calculation are set with the SET SIMULATION PARAMETERS function. In the default mode, the confocal Fabry-Pérot has a 1 m cavity, with mirrors of equal reflection coefficients of 84.5 %, and is used in a transmission mode.

In setting the parameters of the FP, the user should remember that, to accelerate and simplify the calculations, the sampling step is determined by the

length of the cavity. At the default value, this sampling step is equal to 3.34 nsec.

4.1.5 Load simulation data from a file

In this program, we have three types of data: laser pulse shape, displacement and signal of the FP. The data can be saved in a file and retrieved from a file. This function is used to retrieve previously computed simulations. The program directly determines what type of data is reloaded. To modify a parameter, i.e. the directory name or the file name, simply move the cursor with the UP and DOWN keys to the appropriate parameter and press ENTER. Notice that the directory name must end with the backslash (\) character. To load the file, press the ESC key. If the file is loaded, the program will plot the data as function of time. If an error has occurred, an error message explaining the problem will be displayed in the message box (top of screen).

4.1.6 Load a pulse shape from an UDASP file

With this program, a simulated signal can be calculated for an actual laser pulse shape. This function permits the user to transfer data from a file in the UDASP acquisition system format[4] to the program. Since our system has three different types of data, the user must specify what type of data is being loaded. All three types of data can be loaded. It should be noted that the UDASP data array has 1024 data points while our program works with a 2048 points data array. When loading the data, this function interpolates the missing values.

There is no processing of data performed by this function. The data is accepted as it is. Any modification to eliminate noise or a dc offset must be performed prior filing of data with the UDASP software.

4.1.7 Save simulation data into a file

This function places in file the data of a simulation. The user must specify what type of data in memory is to be saved. Only the selected type is recorded in a file. To select the type or modify the directory and/or file name, the user proceeds as with the LOAD FILE function. With the selected data, the function also save the parameters of the simulation as set by the SET SIMULATION PARAMETERS function. Since computation of the laser pulse is generally rapid, we advise the user not to file pulse shape data. Notice that the data are stored

in a binary format and cannot, therefore, be read by any other program without prior processing.

4.1.8 Save simulation data into an UDASP file

This function files the data as the SAVE SIMULATION function but in the file format of the UDASP acquisition system[4]. This allows the user to transfer simulations to the UDASP system for comparison with actual experimental data. As with the SAVE SIMULATION function, the user must specify which type of data is to be filed. Notice that the data is properly scaled to be accepted as a UDASP data array. Also, some of the simulation parameters are placed in the comment portion of the UDASP file.

4.1.9 Set environment

This function allows the user to set the directories accessed by the program. There are three such directories. The first is the font directory containing the font files for the graphics and text presentation of the program. Generally, this directory is the directory where the main executable program is located. The second directory is the one containing the simulation data, i.e. the directory accessed by the LOAD and SAVE functions (both UDASP and normal file). The third and last directory contains the samples files which holds the values of the parameters needed for the computation of the thermoelastic displacement (as set by the EDIT PARAMETER function). To change the name of a directory, the user must move the cursor with the UP and DOWN key to the appropriate value and press ENTER. After writing the new name, the user presses ENTER again to change the value. Notice that the name of the directories must end with the backslash (\) character to be valid.

4.1.10 Set simulation parameters

This is the principal function which lets the user set all the simulation parameters. These parameters can be grouped into three categories: laser pulse parameters, experimental conditions, and Fabry-Pérot parameters.

The first one, which gives the laser pulse parameters, defines the pulse shape of the heating laser. Three shapes have been implemented. The first one is the exponential shape given by equation 18. The rise time is then defined as the time τ for which the pulse acquires its maximum value. The second shape is the gaussian shape given by

$$F(t) = \Phi_0 e^{\left(\frac{t-3\tau}{\tau}\right)^2} \qquad (23)$$

In this case the rise time τ corresponds to the pulse 1/e half-width. Notice that the maximum of the pulse is set at $t=3\tau$. Finally the third shape is DATA, in which the pulse shape is obtain from an UDASP file and generally corresponds to an actually acquired pulse shape. The dc level and any spurious signal should be eliminated before transferring the data to the simulation program since no processing of this data is made by the program.

The energy of the laser pulse is calculated by integration of the pulse shape. The energy and the peak amplitude are linked; if the user changes one of these values, the program automatically computes the corresponding value. For the DATA type pulse shape, no computation of the energy or the peak amplitude is performed. The user must enter the experimental values to obtain a valid simulation. Finally, the spot size of the heating laser is required. This parameter is used to compute the energy density at the surface of the sample. The calculation is made by considering uniform light intensity distribution over the spot size.

The second group of parameters describes the experimental conditions. They include the constituents of the sample, the top layer thickness and the observation depth. The layer and the substrate are identified by the name given to their appropriate parameter file name (given in the EDIT PARAMETER function). The observation depth for remote sensing of oil on water is always zero, since we are observing the surface displacement of the sample. However, the program can also be used to calculate the displacement of the back surface of a two layers system. In this case, the observation depth would be equal to the thickness of the substrate.

The final group of parameter are the Fabry-Pérot parameters. These are the cavity length, the mode of operation, the reflectivity of the mirrors, the offset from resonance, and the probe beam wavelength.

The user should remember that the FP signal is calculated by direct complex summation as indicated by equation 20. To speed up computation, the time scale is set by the time delay $\tau=e/c$. Therefore, the cavity length determines the sampling step.

The simulation can be performed for three different operation modes of the confocal FP: the symmetrical transmission mode, the symmetrical reflection

mode, and the non-symmetrical reflection mode. In the transmission mode, the transmitted signal of a symmetrical confocal Fabry-Pérot is calculated. Symmetrical means end mirrors of equal reflectivity. In the symmetrical reflection mode, the reflected signal is calculated. In the non-symmetrical reflection mode, the reflected signal is calculated for a back mirror reflectivity of 1 (total reflection).

The reflectivity of the mirrors can be set either directly by changing their values or by setting the finesse. The finesse of a Fabry-Pérot is given by

$$f = \pi \frac{\sqrt{R_1 R_2}}{1 - R_1 R_2} \qquad (24)$$

where R_1 and R_2 are the reflectivity of the front and the reflectivity of the back mirror, respectively.

Similarly with the energy and peak amplitude of the laser pulse, when *either reflectivity or finesse are changed, the program automatically computes* the corresponding other values, for a given mode of operation.

Finally the offset from resonance parameter expressed as a fraction of the optical bandwidth (equal to the free spectral range divided by the finesse) should be entered. Note that it is generally set at 0.5. The wavelength of the probe beam *of the laser-ultrasonic system we are using is* 1.06 μm *(YAG laser).*

To modify the value of a given parameter, the user moves the cursor to the position of the parameter with the UP and DOWN keys and presses ENTER. The user then enters the new value in scientific notation with appropriate units (shown on the screen) and presses ENTER again to change the value. Some parameters, such as mode of operation of the FP and pulse shape, can only take well defined values. For these parameters, pressing ENTER will automatically change the present value to the next one allowed. The user must then keep on pressing ENTER until the desired value is displayed. To accept all the parameters and return to the main menu, the user presses on the ESC key.

4.1.11 View simulation

This function displays a chosen type of data on the screen. It allows to recall data between simulation steps. To select a particular type of data, press ENTER until the appropriate type is displayed, then press the ESC key. The program does not verify if the requested data has actually been computed prior

to this call. If no computation has been perform, the program will plot zeros for all values of time.

4.1.12 Graphic functions

For each display of simulation data on the screen, the user can access several graphic functions with the control keys. The F1 key displays a cursor on the screen. This cursor can be move with the LEFT and RIGHT keys or with the CONTROL-LEFT and CONTROL-RIGHT keys (faster movement). To return to normal mode, the user must press ENTER.

The F2 key changes the time interval displayed for all subsequent plots of data. The user must enter the new maximum and minimum time values. The program verifies for inversion (maximum lower then minimum) or for aberrant values (maximum greater then maximum sampled point or minimum lower than zero). To return to full scale, the user must enter for the maximum time any value greater than the maximum sampled point. Generally, a maximum value of 1 sec is sufficient.

Finally, the F3 key displays the setup parameters for the plotted data. To return to normal mode, the user must press ESC.

4.2 Example of a typical simulation session

After reviewing the different functions of the program, we now give an example of its use by calculating the laser-ultrasonic response for a sample composed of a 1 mm thick oil layer on top of water. When the program as been engaged from the DOS operating system, the screen should look like figure 3. Select the EDIT A SAMPLE FILE by pressing ENTER with the cursor (box) set as in figure 3. Enter the name "oil" for the NAME OF THE SAMPLE parameter. After pressing ENTER, the values of the parameters for an oil sample should appear on the screen as shown in figure 4. Any parameter value can be changed if needed. If the values are correct, press ESC to return to the main menu, and press ENTER again to return to the EDIT function. In the EDIT function, enter the name "water" for the NAME OF THE SAMPLE parameter, and verify that the displayed values are identical to those given in figure 5. If it is the case, press ESC. At this point, we have two sample files containing the parameters for oil and water. We must now set the conditions of the simulation. Select the SET SIMULATION PARAMETERS. In the EDIT SETUP PARAMETERS mode (figure 6), set the finesse of the Fabry-Pérot

to 10. The screen should now look like figure 6 (if not, change the non-corresponding values). The simulation is set for a t*exp(-t) pulse shape with a rise time of 100 nsec, a pulse energy of 10 mJ and a spot radius of 3 mm, for a sample of 1 mm of oil on top of water, and for a Fabry-Pérot in a transmission mode with a finesse of 10. Press ESC to return to the main menu.

We can now run the program. First, the pulse shape of the heating laser can be calculated by selecting the COMPUTE LASER PULSE function. The result is shown in figure 7. After pressing ESC to return to the main menu, we compute the thermoelastic displacement by selecting the COMPUTE THE THERMOELASTIC DISPLACEMENT function. The result has been shown in figure 1. Notice that we have an echo arriving from the interface at a time t=1.538 µsec (use the cursor of the F1 key to determine the time of arrival). After pressing ESC to return to the main menu, we compute the signal of the Fabry-Pérot by selecting the COMPUTE THE RESPONSE OF FABRY-PEROT function. The result has been shown in figure 2. We have now completed our simulation. At this stage, we can save the results in a file by selecting the SAVE THE SIMULATION function (figure 8). Finally, to exit from the program, press ESC in the main menu. This erases the screen and sends control back to the DOS command system.

5 APPLICATION TO THE ANALYSIS OF OIL THICKNESS MEASUREMENT BY LASER EXCITATION AND FABRY-PÉROT DETECTION

In this section, we are applying the program which has been developed to the analysis of the problem of oil thickness determination with laser-ultrasonics. This program will allow us to optimize the operating parameters in order to obtain the best determination accuracy. Thickness is determined by a cross-correlation technique[5] which, because of the weak acoustic reflectivity of the oil-water interface, is applied between the derivative of the initial surface pulse and the echo from the oil-water interface.

Using the program, we first analyze the effect of the finesse and the mode of operation on the determination of the delay. The study is limited to three modes of operation: the symmetrical transmission (ST) mode, the symmetrical reflection (SR) mode and the non-symmetrical reflection (NSR) mode. These modes of operation have been defined in section 4. We also study the Fabry-Pérot signal as function of the pulse energy of the heating laser. Our thermoelastic model clearly shows that the amplitude of the displacement is directly

proportional to the amplitude of the heating pulse, hence to the energy of the pulse. However, the response of the Fabry-Pérot is not a linear function of displacement. This non-linearity may impede the observation of the signal for strong or rapid displacements and may affect the result of the cross-correlation.

The various simulations we have made consider a 1 mm thick oil layer on top of water (parameter values given in table 1). The heating laser is a TEA CO_2 laser (10.6 μm wavelength) with a pulse shape of the form t*exp(-t) and a rise time of 100 nsec. Such a pulse shape is typical of such lasers and close to the shape of the laser used in the laboratory. For the study as function of finesse, the pulse energy is set at 10 mJ with a spot radius of 3 mm, i.e. the energy density is 0.035 J/cm^2. For the study as function of laser energy, the finesse is set at 10 independently of the mode of operation.

At the end of this section, we also address the problem of the determination of the thickness of thin layers.

5.1 Signal and precision of the thickness determination as a function of finesse

The purpose of this study is to establish the optimum conditions for measuring the time delay between the first echo and the surface pulse by a cross-correlation technique. First, we study how varies the signal magnitude with finesse. Figure 9 shows the signal of the FP in a ST mode for different finesse f. As finesse increases from 5 to 50, we notice that the height of the first echo increases (at t≈1.5 μsec), as well as the height of the initial surface pulse (t=0 to 1 μsec). This increase in height produces an increase of sensitivity. We also notice that the echo is slightly shifted and that its width increases, particularly for f=100. This increase in pulse width corresponds to an increase of the storage time of the FP cavity and to a reduction of the detection bandwidth at higher finesses.

The mode of operation affects also the detection bandwidth. It is known that the bandwidths of the reflection modes (NSR and SR) are generally larger than that of symmetric transmission mode (ST), at equal finesse (better responsivity at high frequencies). The NSR mode has also a lower responsivity at low frequencies than the ST and SR modes. Figure 10 shows the signals for the three different modes. We notice that the echo is much sharper in the NSR mode. It should be noted that, although the surface signal is apparently narrower for the NSR mode, in all cases the initial surface displacement extends to about

1 µsec. This corresponds to a recovery time of the cavity of ≈1 µsec which is the same for the three modes of operation for the same finesse.

To study more clearly the effect of finesse on the signal, we have isolated the first bipolar echo from the interface in the signal and calculated the peak-to-peak amplitude for each mode of operation. To use the cross-correlation method, it is necessary to identify the presence of an echo. Each echo can then be isolated by using a temporal window. Obviously, the larger is the peak-to-peak amplitude of the echo, the easier it will be to identify it. Figure 11 shows the peak-to-peak amplitude of the echo as function of finesse and mode of operation. Each mode shows a rapid increase. For low finesses (f<20), the SR and ST modes are almost equivalent. As finesse increases (f>20), the best operation is obtain with the NSR mode.

Actually what matters to identify an echo is the signal-to-noise ratio of this echo and we should therefore study the impact of noise. The laser-ultrasonic system is generally shot noise limited. This means that the noise level is proportional to the square root of the light intensity received by the optical detector located at the transmission or reflection sides of the Fabry-Pérot (depending on the mode of operation). This level depends upon the operation mode for a given intensity of the probe beam. Noise is larger for NSR mode, since all of the light is reflected, than for symmetrical modes where only a portion (either transmitted or reflected) is actually received by the detector. To determine the theoretical signal-to-noise ratio (SNR), we have added to the model white noise proportional to the square root of the mean detector level at the FP output. The proportionality constant is adjusted in order to have a SNR of 10 for the ST mode with a finesse of 10. The SNR is calculated by dividing the maximum value of the power spectrum of the signal by the power spectrum of the white noise. Figure 12 shows the SNR of the signal as function of finesse and mode of operation. For low finesses (f<20), the SNR is best with the ST mode. At these finesses, the peak-to-peak amplitude of the symmetrical modes are almost equivalent but the noise level is much smaller for the ST mode then the SR mode. For high finesses (f>20), the best SNR is obtain with the NSR mode. The increase in peak amplitude for the NSR mode rapidly overcomes the higher level of noise for this mode.

Identifying the echoes is only a first step of the thickness determination process. These echoes are then used to determine the time delay by cross-correlation. It can be shown[6] that the error in the estimation of the delay by cross-correlation between two signals is given by

$$\sigma_{error} \leq \frac{1}{\sqrt{2T\int_0^{\infty}(2\pi\nu)^2 \frac{|\gamma(\nu)|^2}{1-|\gamma(\nu)|^2}\,d\nu}} \qquad (25)$$

where T is the time window (sec), ν is the acoustic frequency (Hz) and $\gamma(\nu)$ is the coherence function of the two signals. It can also be shown that this error depends upon the SNR and the bandwidth of the signal[7]. In fact, in the case of low SNR, this error can be written as

$$\sigma_{error} \leq \sqrt{\frac{3}{8\pi^2 T}}\,\frac{1}{SNR}\,\frac{1}{\sqrt{\nu_2^3-\nu_1^3}} \qquad (26)$$

assuming that the signal and the noise power spectra are constant over the band extending from ν_1 to ν_2 (Hz). It can clearly be seen that an increase in SNR and a larger bandwidth will result in a smaller theoretical error.

We cannot use directly equation 25 since we do not have an analytical expression for the coherence function $\gamma(\nu)$. Consequently, we have to estimate the error numerically. The coherence function is obtained by calculating

$$|\gamma(\nu)|^2 = \frac{C_1(\nu)\,C_2(\nu)}{[C_1(\nu)+N_1(\nu)]\,[C_2(\nu)+N_2(\nu)]} \qquad (27)$$

where $C_1(\nu)$ and $C_2(\nu)$ are the power spectra of respectively the first and second signals, and $N_1(\nu)$ and $N_2(\nu)$ are their corresponding noise level. The power spectra are obtained directly by calculating the square of the amplitude of the numerical fast Fourier transform for each signal. It should be noted that since we are using the derivative of the surface pulse to correlate with the first interface echo, the noise power spectrum for the first signal is no longer constant but proportional to the frequency ν. The integral in equation 25 is then numerically estimated using the trapezoidal rule.

With this procedure, we have calculated the theoretical error of the delay measurement as function of finesse and mode of operation for the oil-water sample. The results are presented in figure 13. As expected, for low values of f ($f<20$), the best results are obtained for the ST mode since for these finesses, the SNR is best for this mode of operation (figure 12). At high values of f ($f>20$), the best results are for the NSR mode, again because of higher SNR for this mode.

Equation 25 supposes that the correlated signals are identical signals, i.e. that the signals are simply the same function shifted in time. In the case of the oil-water sample, the cross-correlation is performed between two different signals namely the interface echo and the derivative of the initial surface pulse. For this reason, a systematic error may be introduced.

Figure 14 shows the variation of the delay estimated by cross-correlation of the derivative of the initial surface pulse with the first interface echo as function of finesse and mode of operation. This delay is determined by measuring the position in time of the peak amplitude of the cross-correlation. For a thickness of 1 mm of oil, the actual delay should be t=1.538 µsec. For low finesses, the estimated value is generally independent of the finesse, but depends on the mode of operation. It is also shifted from the actual value. This shift results from the use of the derivative of the surface initial pulse for the cross-correlation. Since the surface pulse shape is different for each mode of operation (as can be seen in figure 10), the effect of its derivative, i.e. the shift, will also depend on the mode of operation. As finesse increases, the shape of the surface pulse is modified (figure 9) and the echo widens. This results in an overlap of the surface pulse and the echo, modifying substantially the result of the cross-correlation. Figure 14 shows that for higher finesse, the worst case is for the ST mode where the estimated delay rises rapidly. However, in practice, since the acoustic velocity of oil is not known with great accuracy, a systematic error of a few percents is not severe.

5.2 Signal versus energy of heating laser pulse

A second approach to increase the sensitivity and the SNR of the technique is to raise the amplitude of the displacement by increasing the energy of the laser pulse. Figure 15 shows the signals given by a FP of a finesse of 10 as function of the mode of operation, the pulse energy being 100 mJ (energy density = 0.35 J/cm^2). If we compare these results with those of figure 10 (pulse energy = 10 mJ), we immediately notice a large increase of the amplitude of the interface echo. Figure 15 also shows a strong non-linearity occurring with the initial surface pulse in transmission and in reflection. In transmission, the increase observed between figure 15 and figure 10 is much less than the ratio of the energies, while in reflection, strong oscillations are observed. It should be first noted that a non-linear behaviour is expected since

the signal variation is limited by the average intensity received by the detector which is equal to 0.25, 0.75 and 1.0 for the ST, SR and NSR modes respectively, for a unitary incident intensity. As the energy of the pulse is increased, the initial surface displacement increases proportionally. The movement of the surface introduces a phase shift of $4\pi u(t)/\lambda$ of the reflected wave (where u(t) is the surface displacement and λ the probe beam wavelength). The Fabry-Pérot add up the multiple delayed waves as indicated by equation 19. As long as the surface displacement variation during the cavity delay time ($=4\tau$, for a confocal FP) is much smaller then $\lambda/8$, the phase shift between consecutive waves in the FP is less then $\pi/2$ and all the waves add up nearly in phase. However, when the displacement variation becomes larger, the waves are no longer nearly in phase and some cancellation occurs which will decrease the signal.

This explanation is valid for the FP used in transmission. In the case of the reflection, it is known that the operation is essentially described by the interference of the superposition of the multiple cavity waves with a wave directly reflected by the front mirror. It is therefore similar to a two-waves or heterodyne detection. In this case, we should expect that a non-linearity and saturation effect starts to occur for a total displacement of $\lambda/8$ and not for a displacement variation of the same magnitude, during a cavity delay time. This is verified in figure 15 and more clearly in figure 16 which shows the first μsec on an enlarged time scale with the corresponding surface displacement. The initial drop in the surface signal starts for a displacement of 0.1321 μm which is about $\lambda/8$. Since we are using the surface pulse for the estimation of the delay, this non-linearity may introduce some error (shift) in the estimate.

The main reason to increase the pulse energy is to increase the peak-to-peak amplitude of the echo. Figure 17 shows this amplitude as function of energy and mode of operation. We notice a steady increase with respect to energy for all modes. The relation is however slightly non-linear because of the non-linear relation between displacement and signal introduced by the Fabry-Pérot.

By adding white noise for each mode, as in section 5.1, we can calculate the theoretical SNR for each case. Figure 18 shows the SNR as function of energy and mode of operation for a finesse of 10. The relation is again non-linear, although barely visible on the figure. The best SNR is observed with the ST mode of operation because of the choice of a finesse value equal to 10 (see figure 12).

Since the SNR increases with increasing laser energy, we should expect that the theoretical error derived from equation 25 rapidly decreases at higher energies. Figure 19 shows the variation of the error, numerically calculated as described previously, as a function of laser energy and mode of operation. Since we have chosen a finesse of 10 where this theoretical error is about the same for all modes (see figure 13), there is no significant difference between modes. As expected, the error decreases rapidly with increasing laser energy.

Finally, figure 20 shows the variation of the delay evaluated by cross-correlation as function of pulse energy and mode of operation. The actual value of delay is t=1.538 µsec. It appears that the non-linearity of the surface pulse does not significantly impede the estimation of the delay and that the systematic error which is observed is not very significant in comparison with the limited accuracy of the acoustic velocity of oil.

It should be noted that the presence of the non-linearity of the surface pulse introduces an oscillatory variation of the numerical cross-correlation. It will be therefore more difficult to determine its maximum in presence of noise.

5.3 Determination of the thickness of thin layers

Until now, our analysis has been limited to oil layers which are sufficiently thick to cause the interface echo to be clearly separated from the surface pulse. In the case of thinner layers, the surface pulse signal may overlap the interface echo making more difficult the use of the cross-correlation technique. Increasing the bandwidth of the system by using the NSR mode might produce a sharper surface pulse. Figure 21 shows the FP signal for the NSR mode as function of the thickness of the oil layer for a finesse of 10 and a pulse energy of 10 mJ. For a thickness of 100 µm, the echo is masked. As we have already mention, the sharper surface pulse for the NSR mode is only an illusion. The surface signal extends to about 1 µsec for all modes. Figure 22 shows the FP signal for the ST mode in the same conditions as figure 21. Again, for a thickness of 100 µm, the echo is masked. So changing mode does not allow us to measure thin samples.

It should be noted that any increase of finesse has the effect to widen the pulse shape. Figure 23 shows the same signal as figure 21 but with a finesse of 80. In this case, the echo cannot even be identified for a thickness of 250 µm.

Therefore, it appears that improvement in minimum measurable thickness cannot be obtained by simply changing the Fabry-Pérot parameters or mode of operation. The key to this problem is to narrow the width of the initial surface displacement pulse, which can be done by decreasing the pulse width of the heating laser. Figure 24 shows the FP signal as function of laser pulse rise time for a pulse shape $t/\tau \exp(-t/\tau)$. With a 10 nsec rise time, which corresponds a 24.5 nsec pulse width, the echo can be observed although there is still some overlap with the initial surface pulse. In this case, estimation of the delay by cross-correlation is possible. In conclusion, the measurement of thin layers requires shorter laser pulses.

5.3.1 Reduction of pulse width by deconvolution

Since the FP signal is composed essentially of a series of spikes convoluted with a function (depending upon the thermoelastic effect and upon the Fabry-Pérot) that widens the pulses, we can eliminate this function by deconvolution and recover, in principle, the initial spikes (echoes). The problem is then to determine this function. A first approach which can be followed is to consider that the thin oil layer has almost no effect on the signal. The signal should then be almost identical to the signal of a sample of water with no oil layer on top. Figure 25 shows the results of the deconvolution of the FP signal for a sample of a 100 µm of oil on top of water by the FP signal obtain on water only (for both cases : ST mode, finesse 10, pulse energy 10 mJ). The deconvolution has been calculated by simple complex division of the corresponding Fourier transforms. We notice that the surface pulse is now almost a spike. Also, the echo is now a very narrow bipolar pulse. Measuring the distance between the maximum of the surface pulse and the maximum of the echo yields a delay of t=0.1534 µsec, when the actual value is t=0.1538 µsec.

A second approach is to consider that even for thin layer, this layer determines the shape of the initial surface displacement pulse. Figure 26 shows the results of the deconvolution of the FP signal of a 100 µm oil layer on top of water by the FP signal of an oil only sample (same conditions as figure 25). We notice that the surface displacement is now a very sharp pulse. The echo is a mono-polar pulse which maximum is precisely (within the time sampling step) at the theoretical delay value. We also observe a new echo at t=0.0769 µsec. This echo is the signal resulting from the direct absorption of the laser pulse in water. Since the oil sample is thin, only a small portion of the laser beam is

absorbed in the oil layer, leaving a significant amount of energy to be absorbed by the water substrate. This absorption then generates a signal which arrives at the surface after propagating through the oil layer, that is at t=0.0766 μsec, as observed.

These results tend to indicate that it is possible to reduce the pulse width by deconvolution. However, we have not yet established the impact of noise on this procedure. Direct deconvolution by complex division produces an amplification of the deconvolved signal for frequencies where the reference signal spectrum is weak. When performed with experimental data, this will generally increase the noise level. A combination of deconvolution and linear filtering could then be used. Additional work is needed using actual experimental data to determine the best combination of reference signal and filter to reduce the width of the echoes by deconvolution.

6 CONCLUSION AND SUMMARY

We have developed a model which describes the thermoelastic generation of ultrasound by laser on a sample made of oil on top of water and which also describes its detection with a confocal Fabry-Pérot. This model has been implemented into an interactive computer program. Such a program will be a very useful tool for guiding development and experimentation, and for interpreting experimental data. With the help of this program, we have been able to draw the following conclusions :

- in the case of sufficiently thick layers giving an interface echo well separated from the surface pulse, the best precision of determination of delay is obtained with the non-symmetrical reflection mode (assuming operation of the Fabry-Pérot in agreement with theory and photon-noise limited detection), although the gain with respect to the other modes is not very large (≤ 2). If étendue is not a limitation, finesse of 20 to 30 would be an appropriate choice. The systematic error was found to be negligible if one takes into account the limited accuracy on the knowledge of oil acoustic velocity.

- non-linearity effects can occur especially with the surface pulse, but they do not affect significantly the precision of determination for thick layers.

This means that, in practice, one should not limit the energy of the laser and try to get as large as possible energy density (below the vaporization threshold).

- layers as thin as 0.2 mm appears measurable with the present system but no further improvement seems possible by varying the Fabry-Pérot parameters. The limitation is caused by the pulse duration. Therefore, the effort should be directed towards the use of shorter pulses. Deconvolution also appears promising, but will require further studies.

REFERENCES

1 **J.-D. Aussel and J.-P. Monchalin**, *Laser-Ultrasonic measurement of oil thickness on water from aircraft : feasibility study*, IMI report, 1990.

2 **J.-P. Monchalin**, *Optical detection of ultrasound*, IEEE Transaction on Ultrasonics, Ferroelectrics and Frequency Control, vol UFFC-33, no. 5 (1986), pp. 485-499.

3 **J.-P. Monchalin, R. Héon, P. Bouchard, C. Padioleau**, *Broadband optical detection of ultrasound by optical sideband stripping with a confocal Fabry-Pérot*, Applied Physics Letters, vol. 55 (1989), pp. 1612-1614.

4 UDASP 1.0, distributed by Ultra Optec Inc, 27 de Lauzon, Boucherville, Québec, J4B-1E7.

5 **D. R. Hull, H. E. Kautz and A. Vary**, *Measurement of ultrasonic velocity using phase-slope and cross-correlation methods*, Material Evaluation, no. 43 (1985), pp. 1455-1460.

6 **C. H. Knapp and G. C. Carter**, *The generalized correlation method for estimation of time delay*, IEEE Transactions on Acoustics, Speech, and Signal Processing, vol. ASSP-24, no. 4 (1976), pp. 320-327.

7 **A. H. Quazi**, *An overview on the time delay estimate in active and passive systems for target localization*, IEEE Transactions on Acoustics, Speech, and Signal Processing, vol. ASSP-29, no. 3 (1981), pp. 527-533.

8 **E. M. Reimer and J. R. Rossiter**, *Measurement of oil thickness on water from aircraft A:Active microwave spectroscopy, B:Electromagnetic thermoelastic emission*, Environmental Studies Research Funds Report No. 078, Ottawa, Ontario, Canada (1987).

TABLE 1

Optical, thermal and acoustic properties of oil and water from Reimer and Rossiter [8].

	Oil	Water
Optical absorption coefficient at 10.6 μm (m^{-1})	1.0×10^4	1.0×10^5
Density (kg/m^3)	8.0×10^2	1.0×10^3
Specific heat at constant pressure (J/kg °K)	2.5×10^2	1.0×10^3
Longitudinal acoustic velocity (m/sec)	1.3×10^3	1.5×10^3
Thermal expansion coefficient ($°K^{-1}$)	1.0×10^{-4}	4.1×10^{-5}

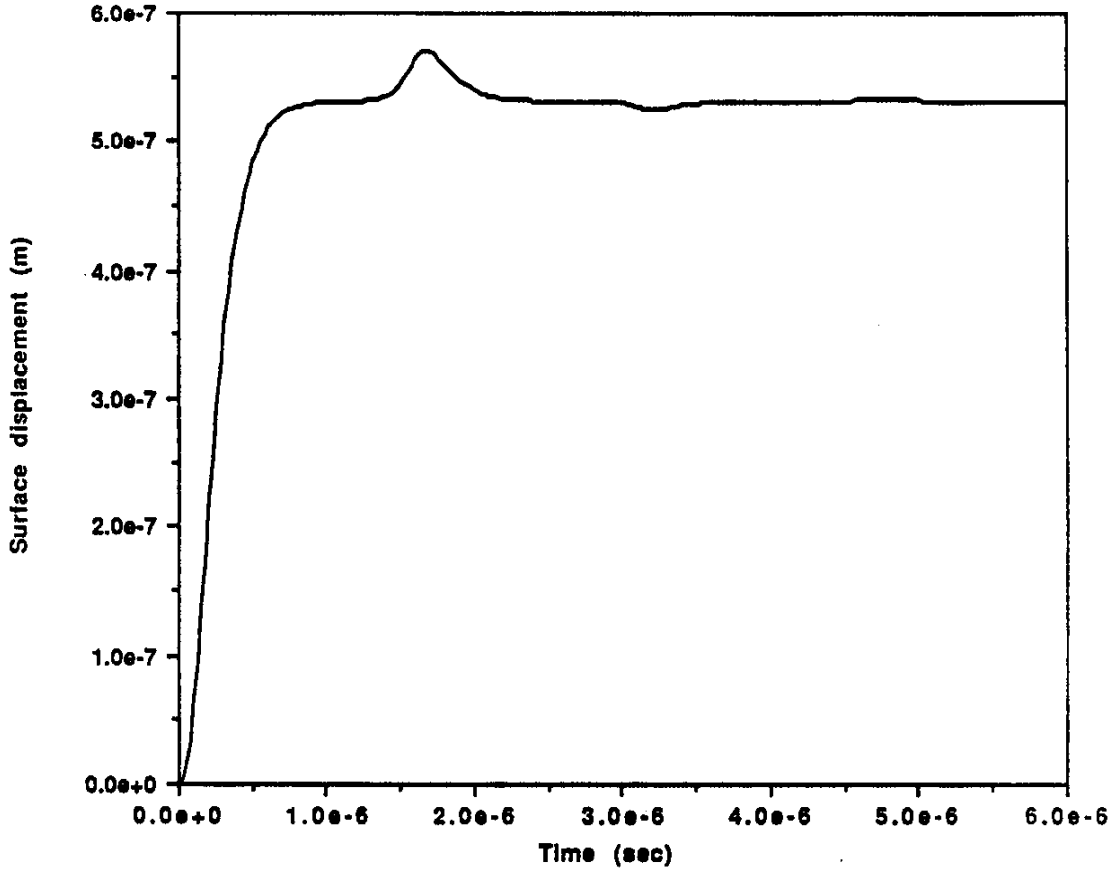

Figure 1 : Surface displacement of a 1mm thick oil layer on water

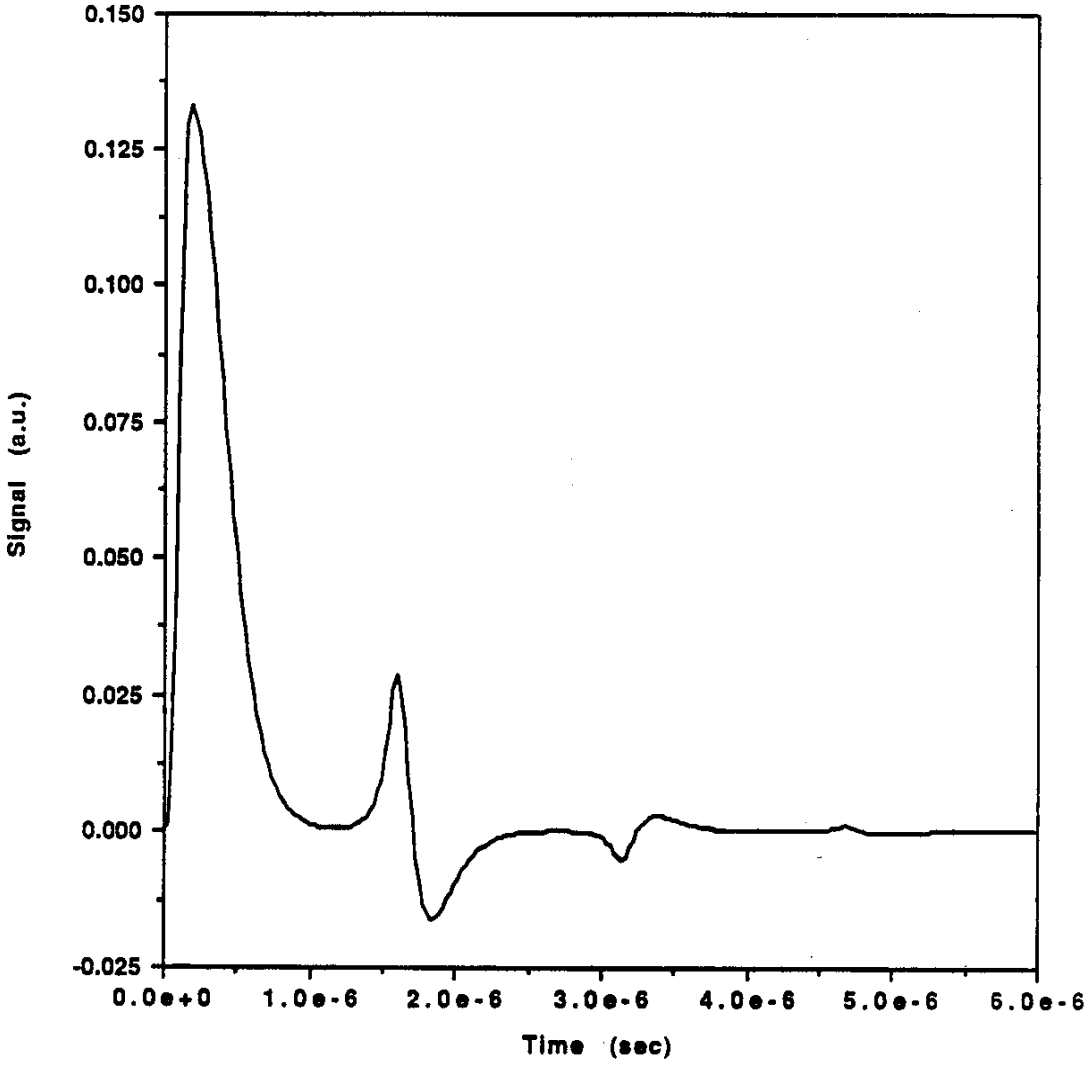

Figure 2 : Signal given by a confocal Fabry-Pérot, ST mode, finesse = 10, pulse energy = 10 mJ

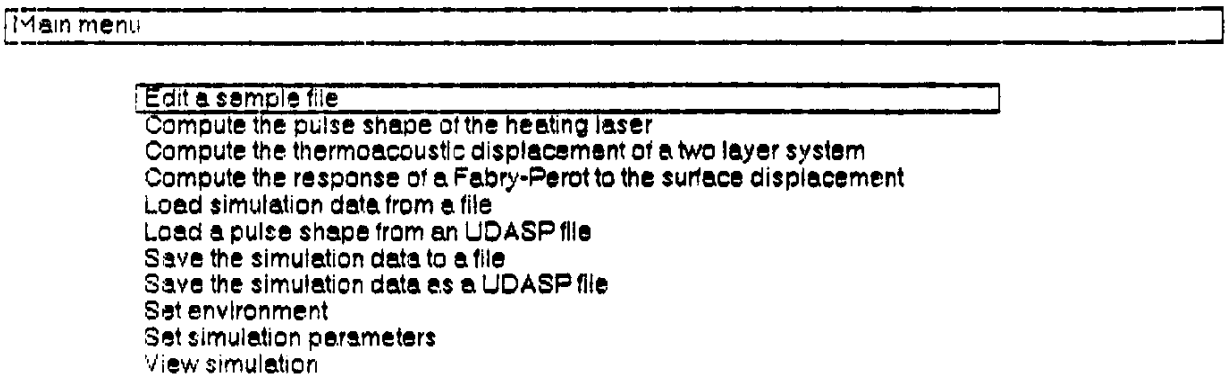

Figure 3 : Main menu of the program

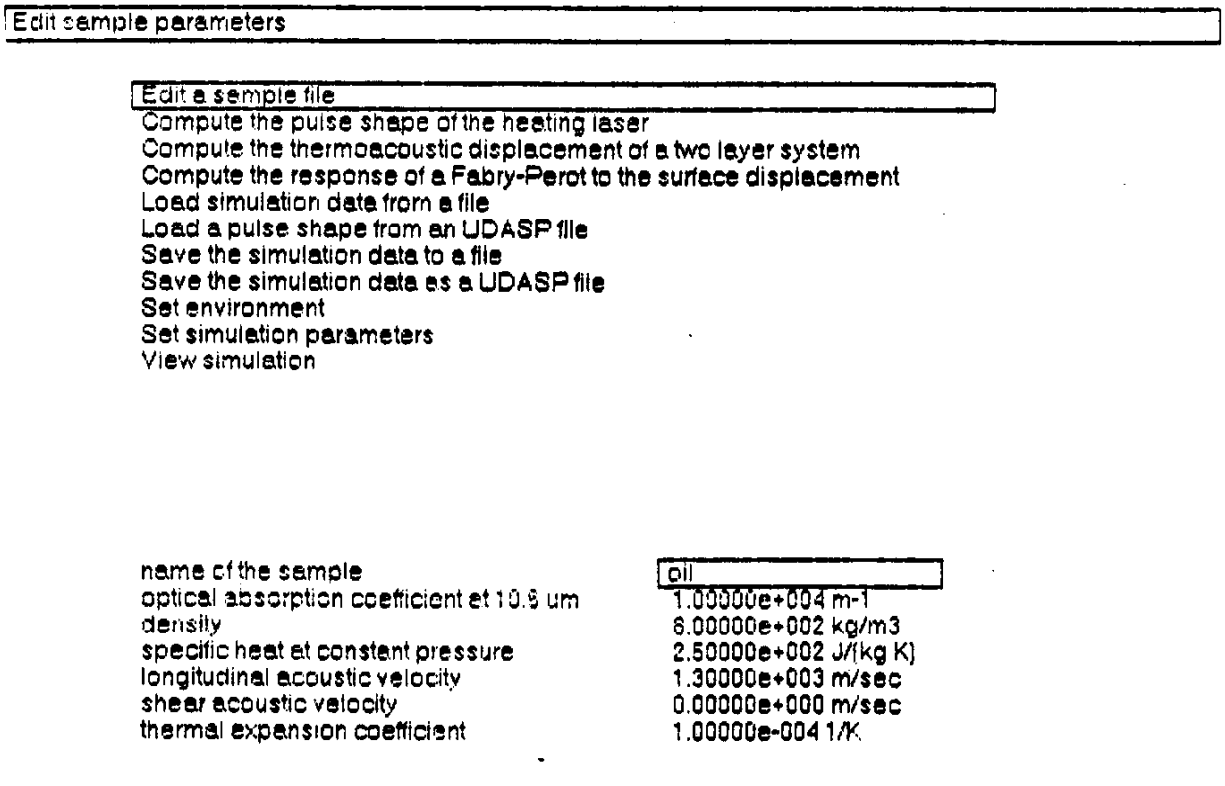

Figure 4 : Editing the parameters of the top layer.

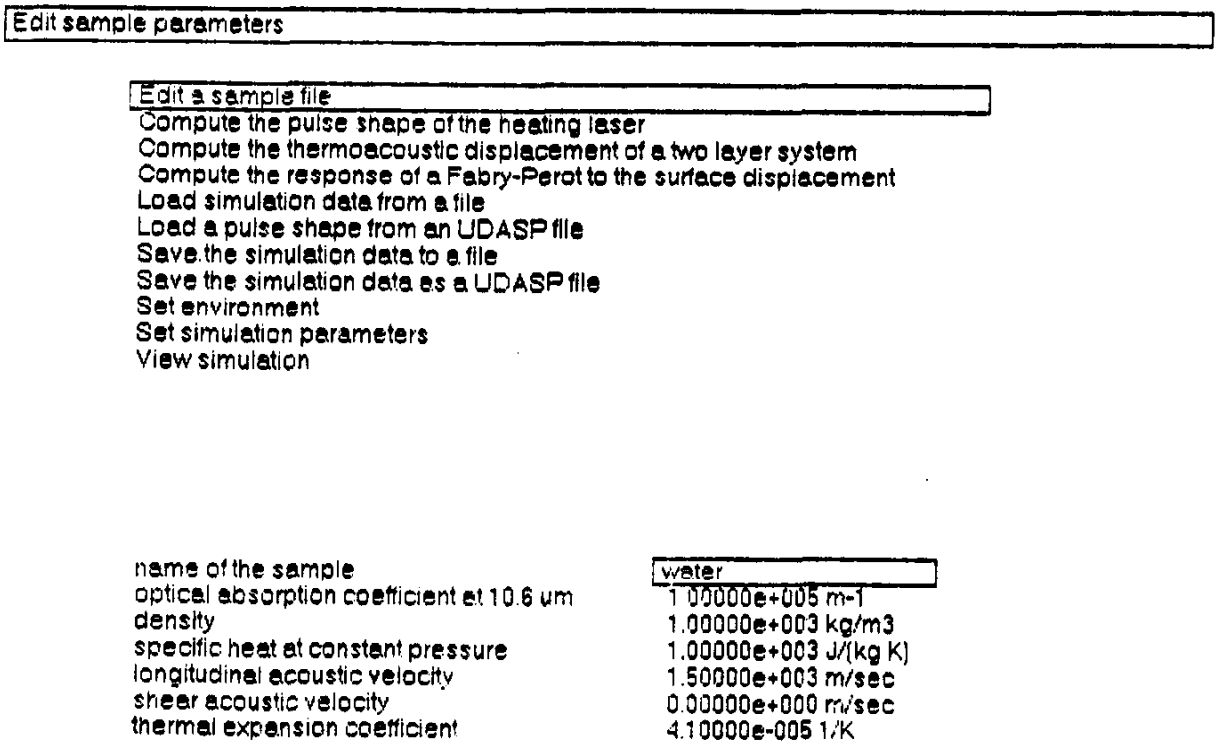

Figure 5 : Editing the parameters of the substrate.

Edit setup parameters

Laser pulse parameters	
shape	t*exp(-t)
rise time	1.00000e-007 sec
energy	1.00000e-002 J
peak amplitude	3.67879e+004 W
radius of laser spot on the sample surface	3.00000e-003 m
Samples parameters	
name of layer	oil
thickness of layer	1.00000e-003 m
name of substrat	water
depth of observation	0.00000e+000 m
Fabry-Perot parameters	
length of cavity	1.00000e+000 m
mode of operation	transmission
reflectivity of front mirror	8.55182e-001
reflectivity of back mirror	8.55182e-001
finesse	1.00000e+001
optical bandwidth	7.49481e+006 Hz
offset/resonnance in bandwidth unit	5.00000e-001
probe beam wavelength	1.06000e-006 m
Sampling parameters	
sampling step	3.33564e-009 sec
total sampled interval	6.82806e-006 sec

Figure 6: Editing the parameters of the simulation.

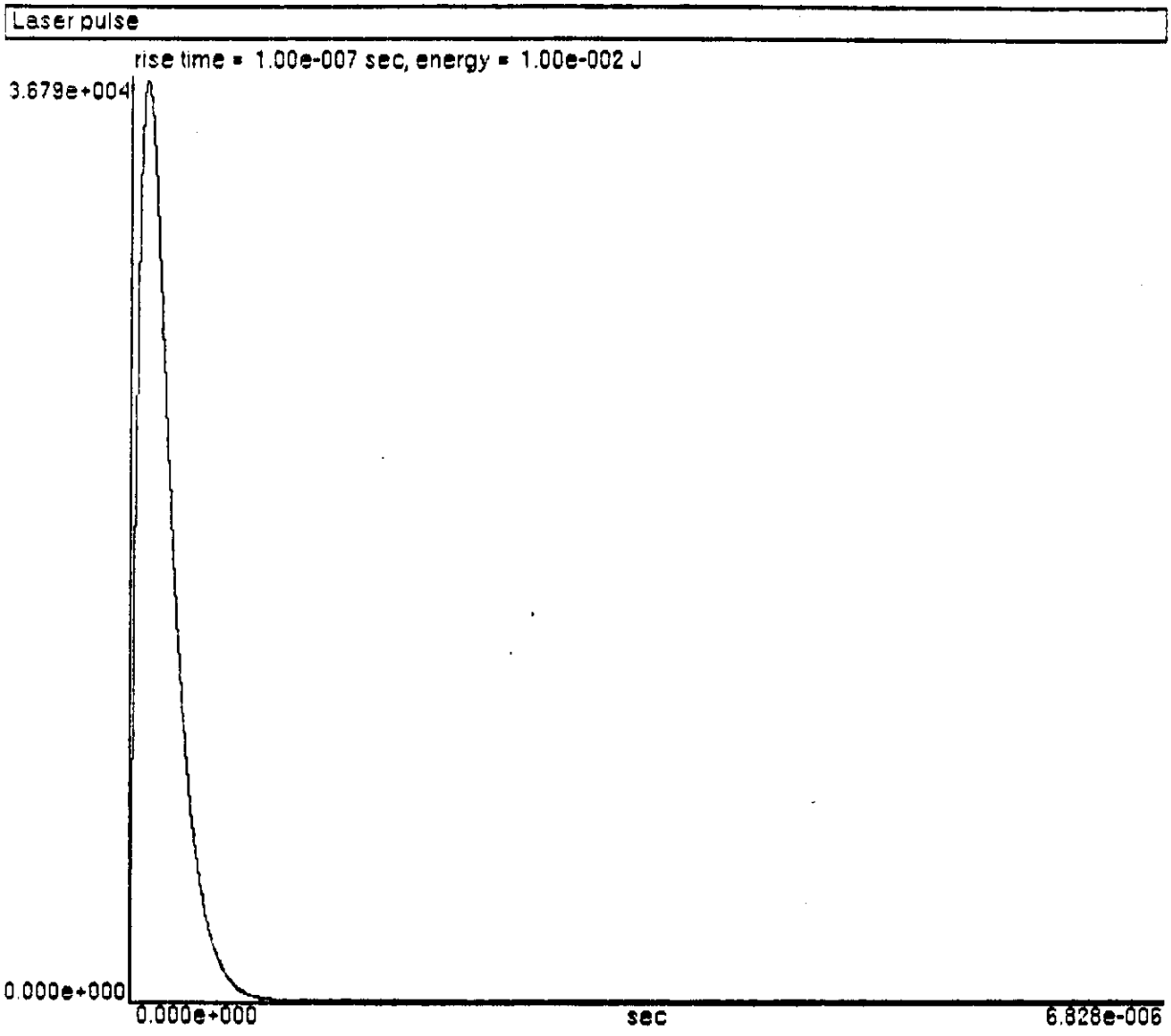

Figure 7 : Display of the theoretical pulse shape $t/\tau \exp(-t/\tau)$ with a rise time of 100 nsec and an energy of 10 mJ.

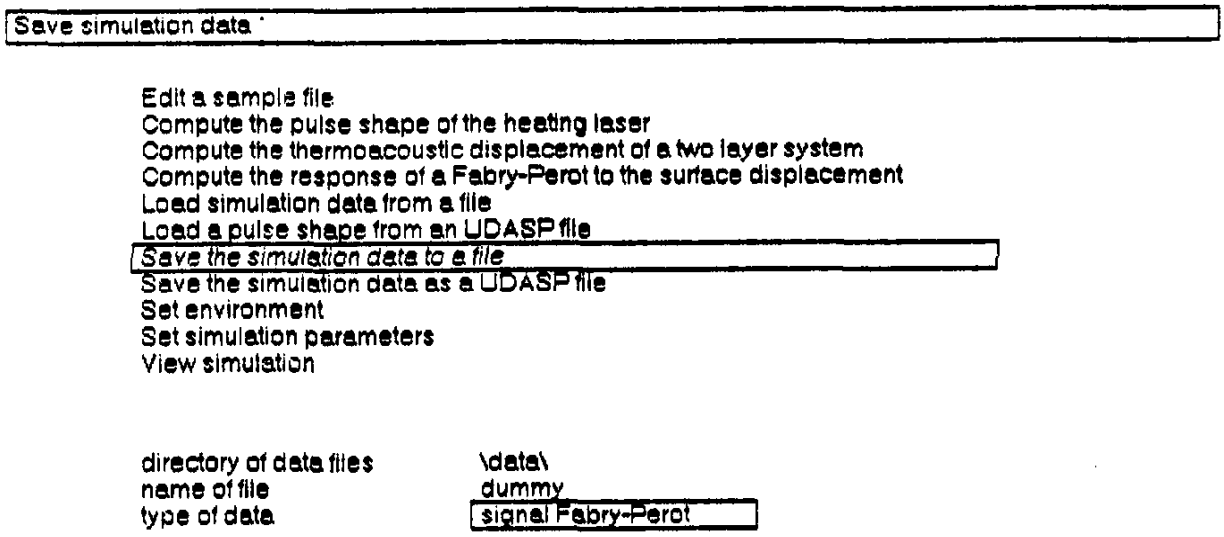

Figure 8 : Saving simulation data

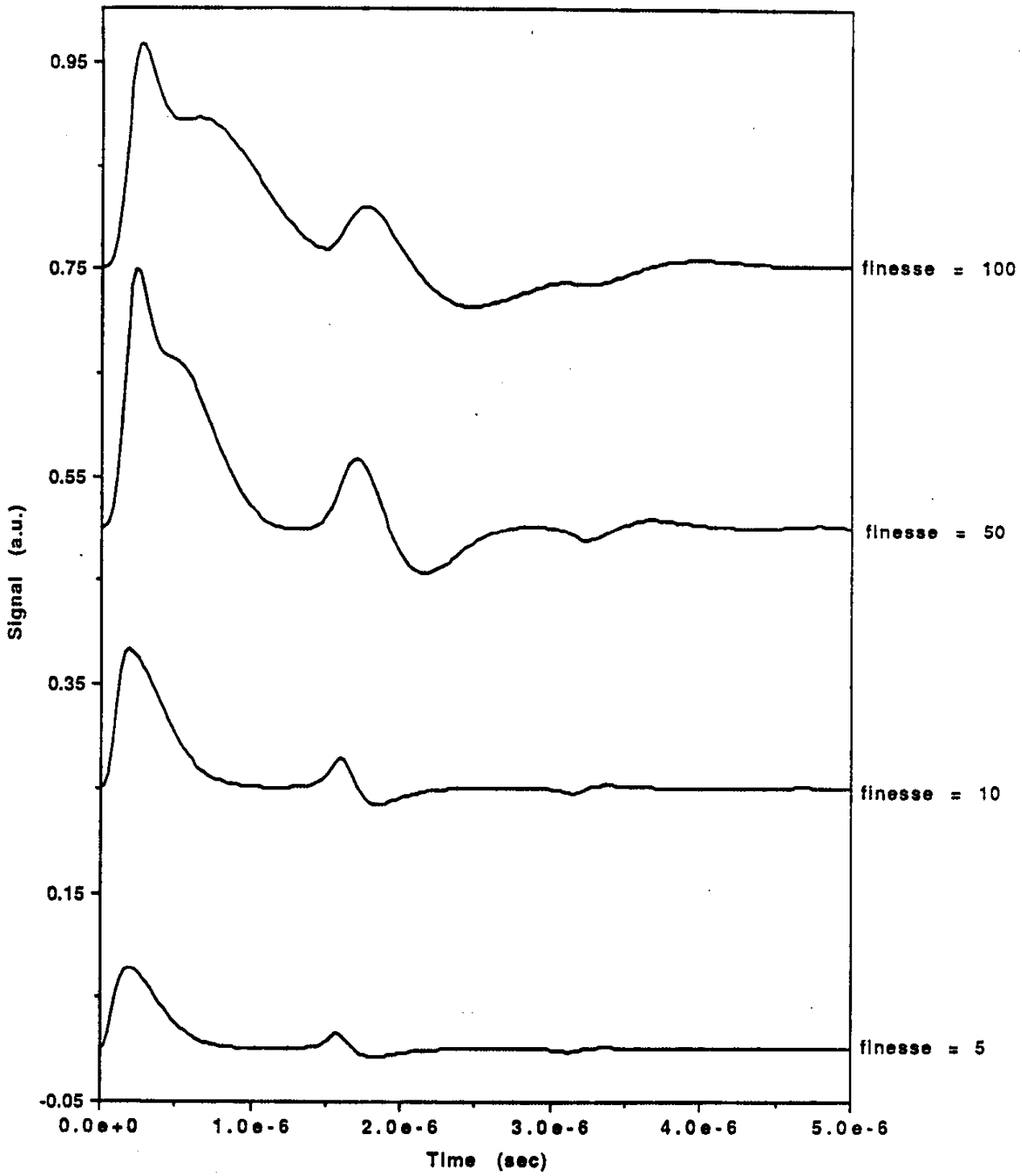

Figure 9 : Variation of signal with finesse for a confocal Fabry-Pérot (1 m long, ST mode)

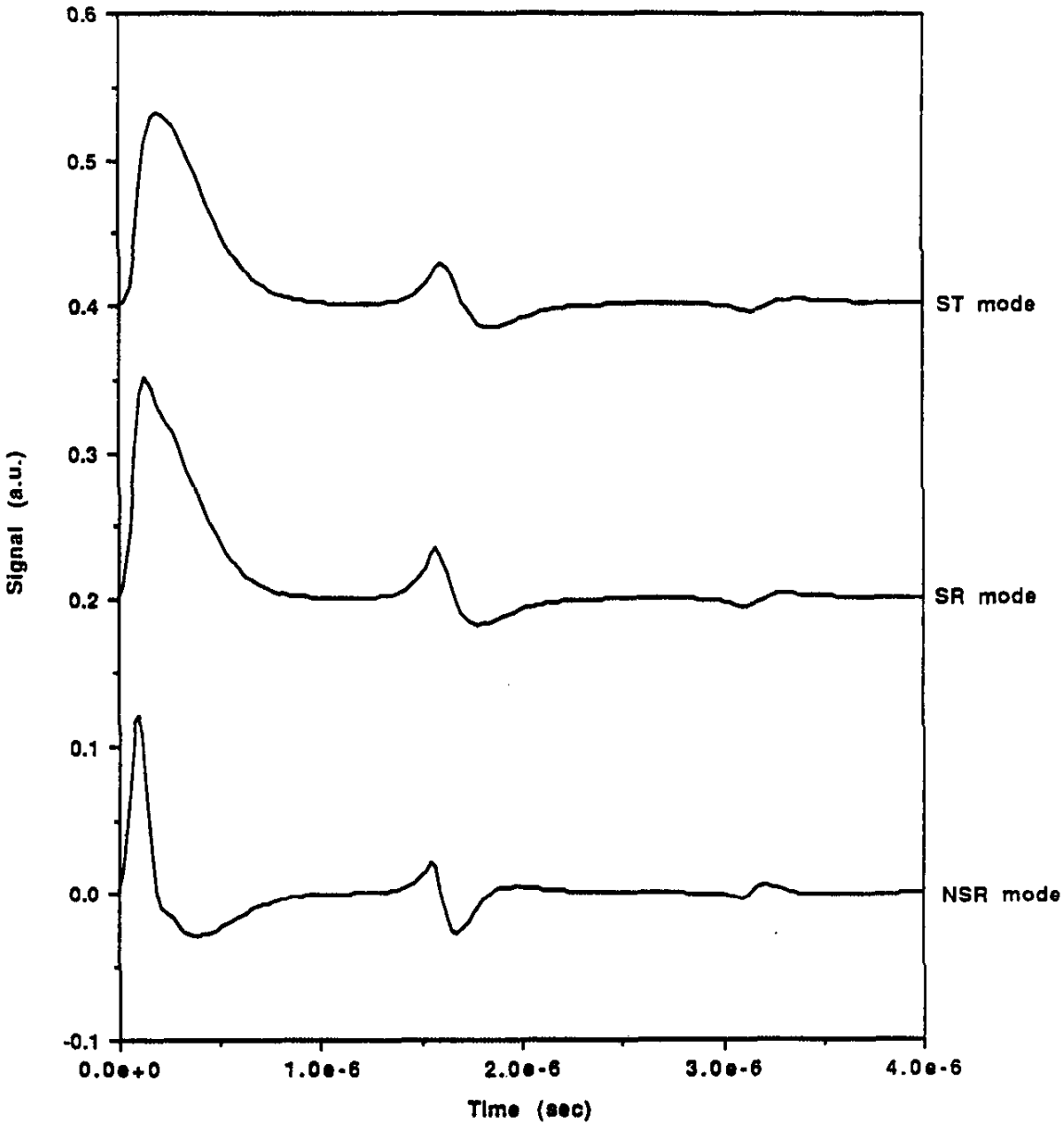

Figure 10 : Variation of the signal with confocal Fabry-Pérot operating modes
(1 m long, finesse = 10)

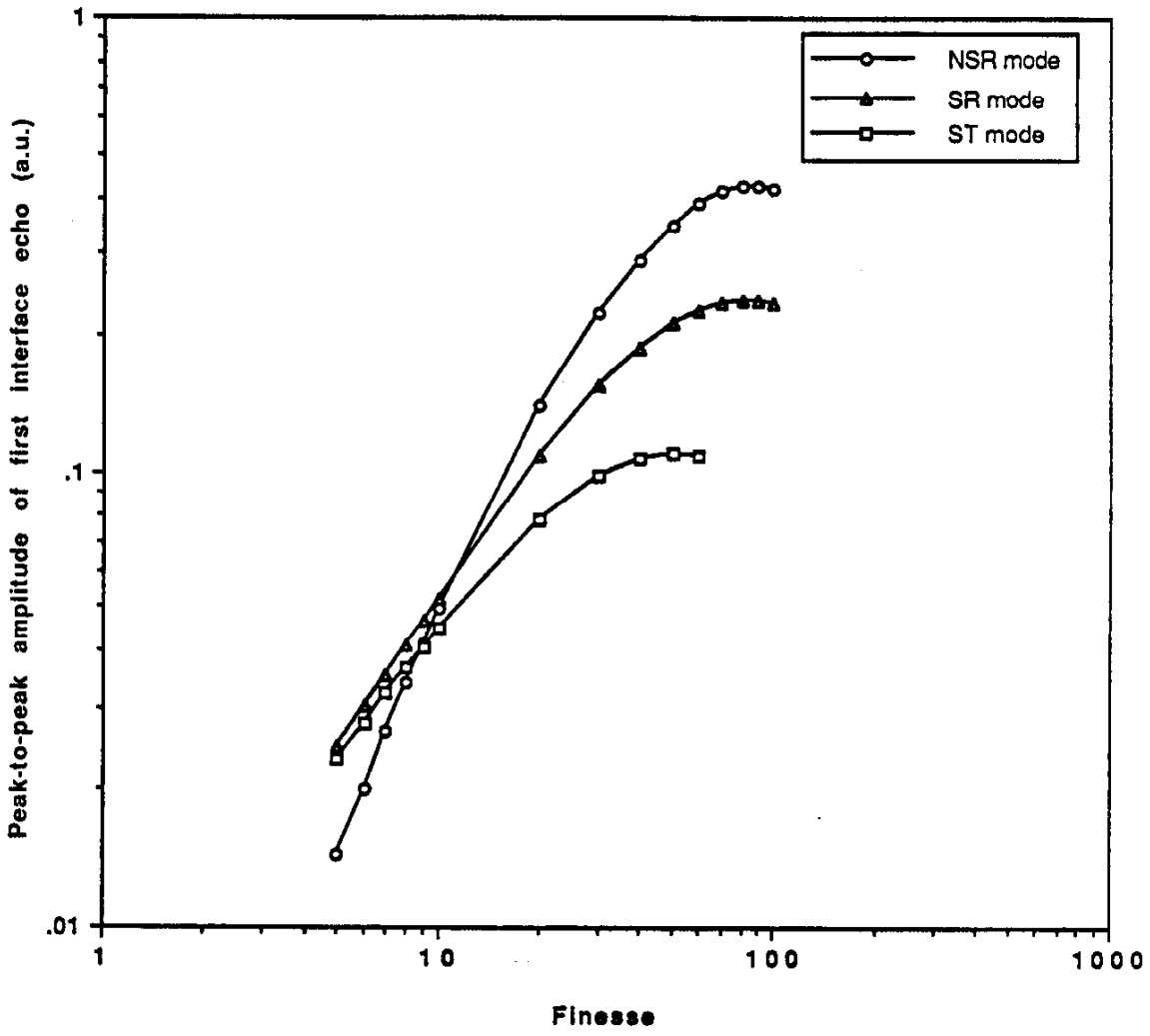

Figure 11 : Peak-to-Peak amplitude of the first interface echo as a function of finesse for three different modes of operation.

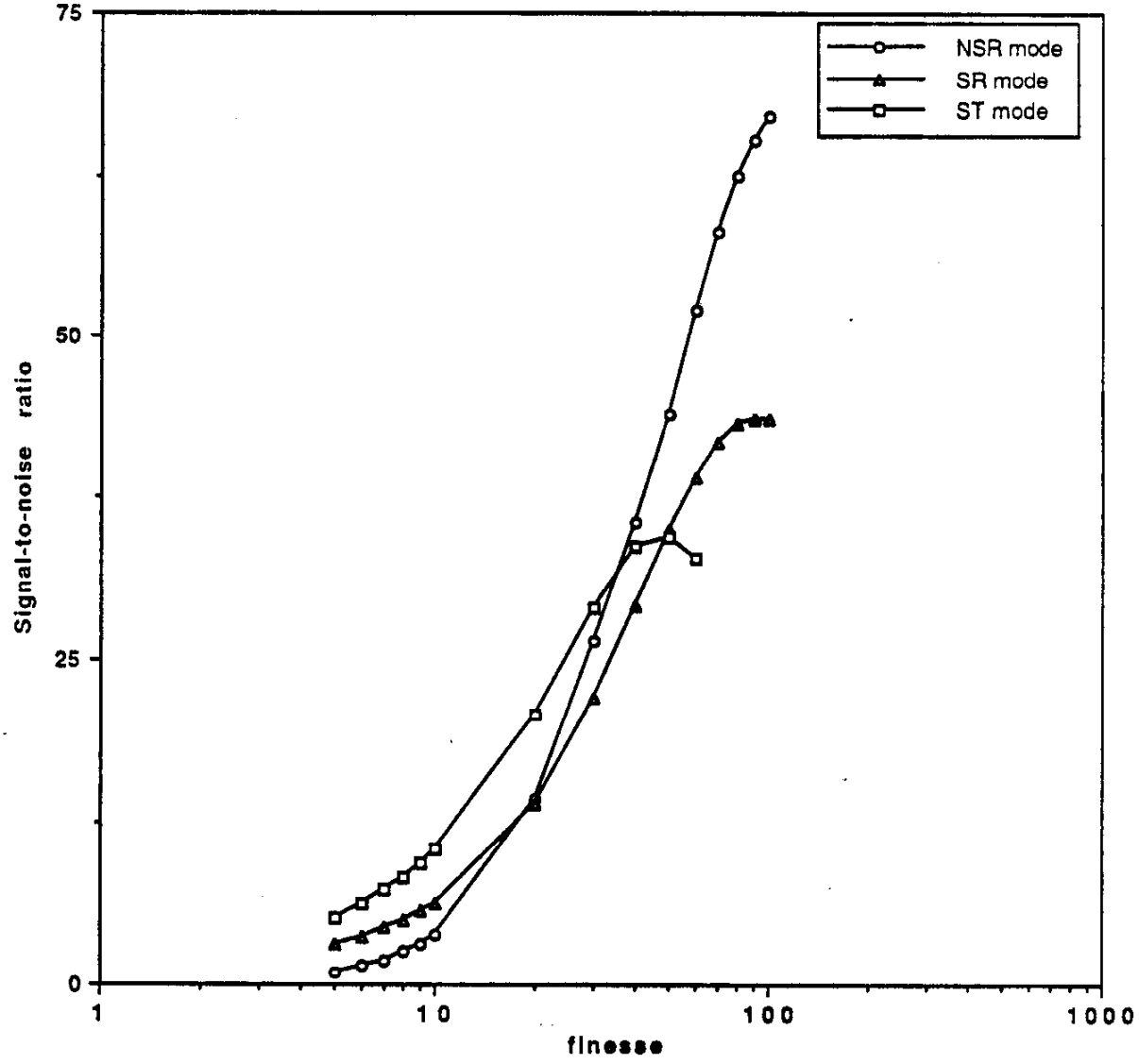

Figure 12 : Signal-to-noise ratio of the first interface echo as a function of finesse for three different operation modes (assuming a SNR of 10 at finesse=10 for ST mode).

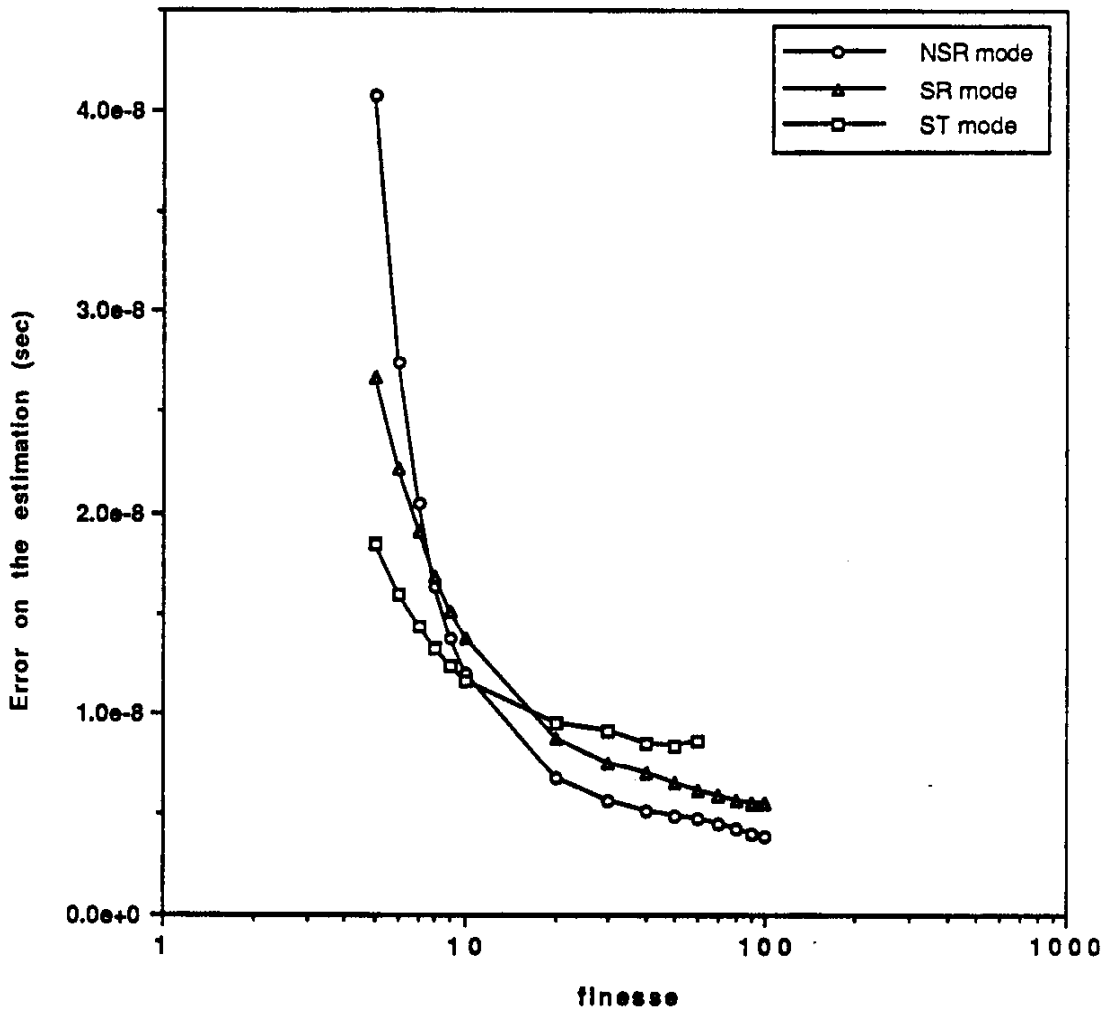

Figure 13 : Theoretical error of the delay determination between the interface echo and the surface pulse derivative by cross-correlation as function of finesse for three modes of operation. (assuming a SNR of 10 at finesse=10 for ST mode)

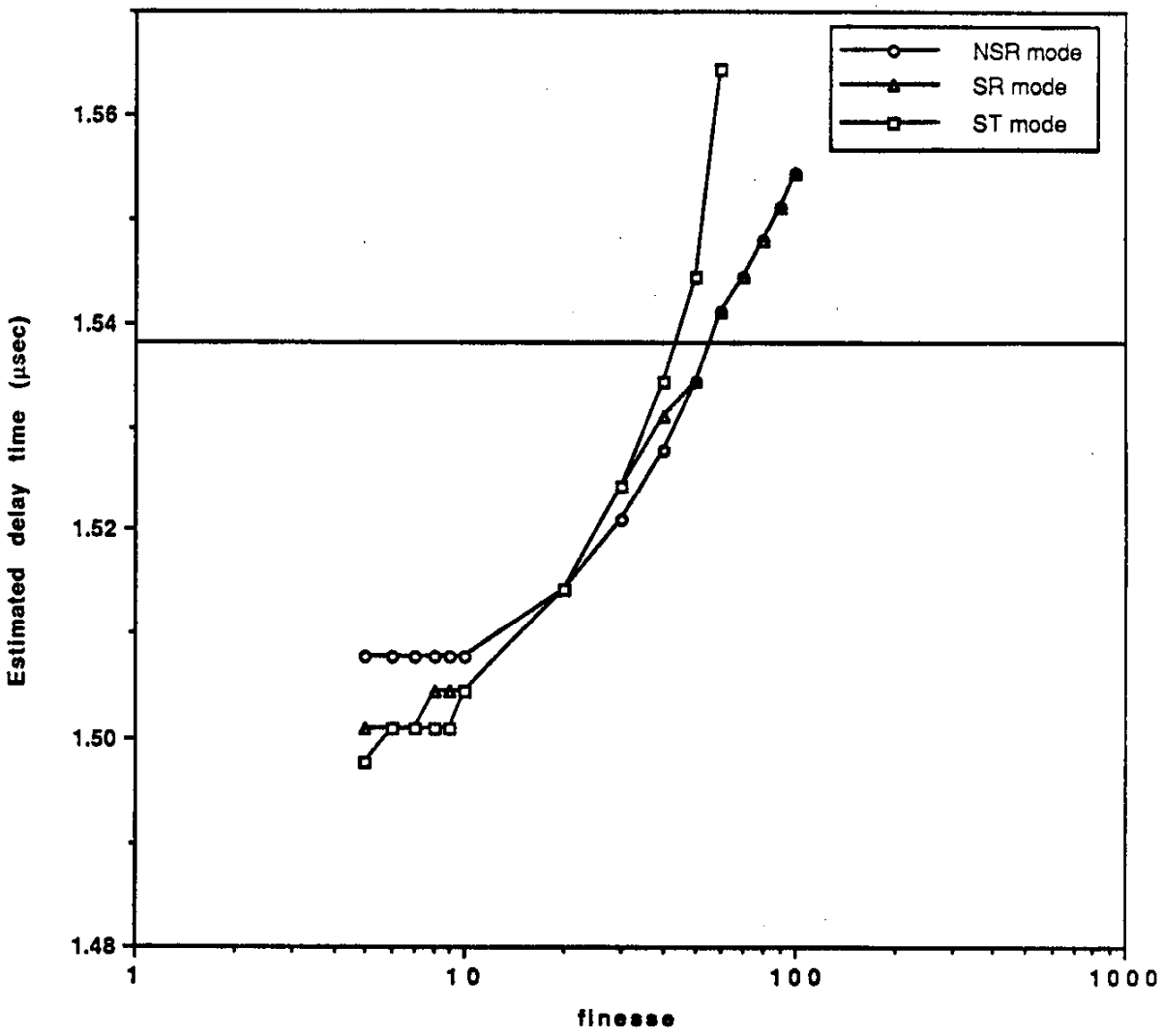

Figure 14 : Estimated delay versus finesse for three modes of operation.
The horizontal line indicates the exact value.

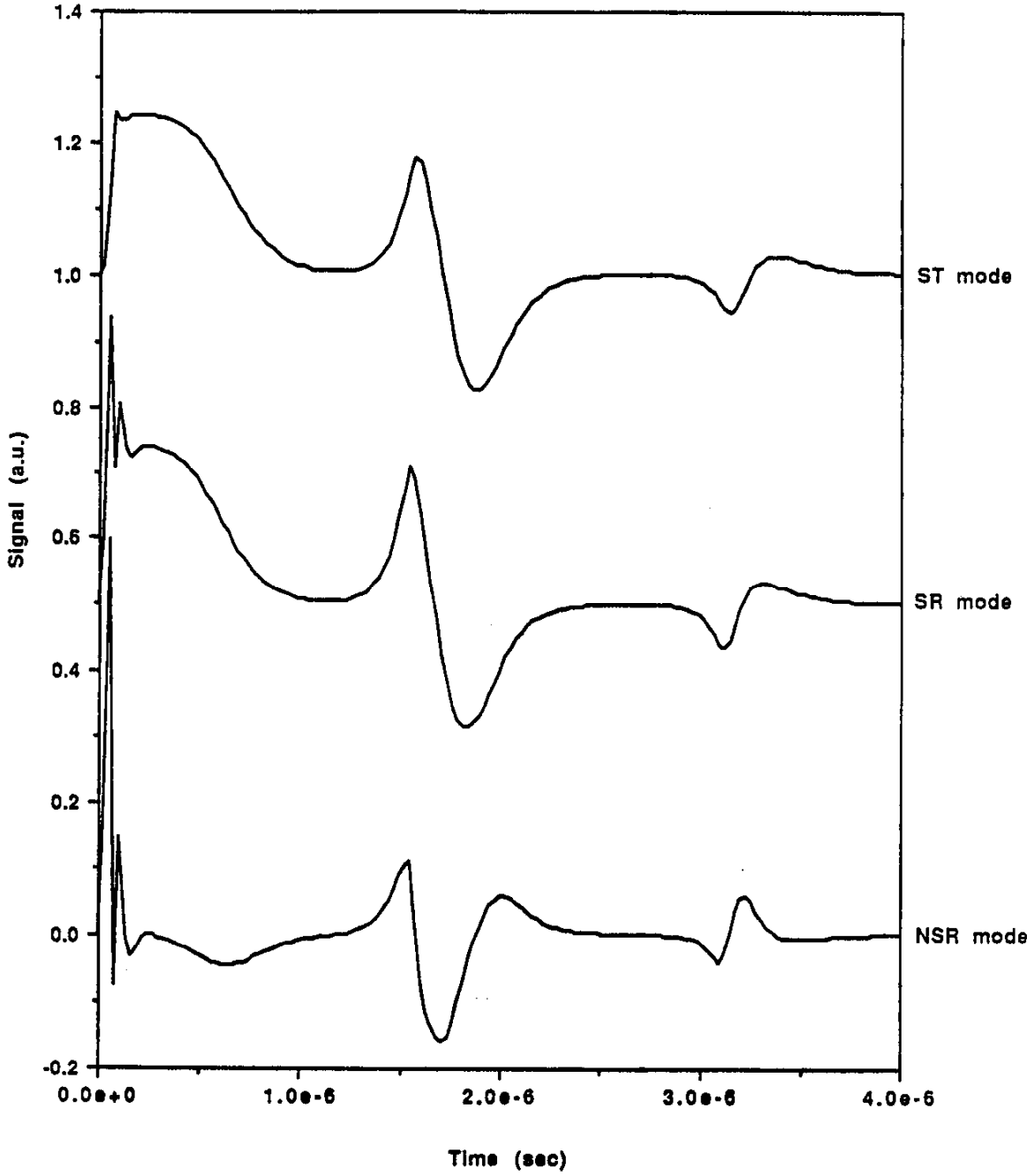

Figure 15 : Signals given by a confocal Fabry-Pérot (1 m long, finesse = 10) in three modes of operation - laser energy = 100 mJ (energy density = 0.35 J/cm)

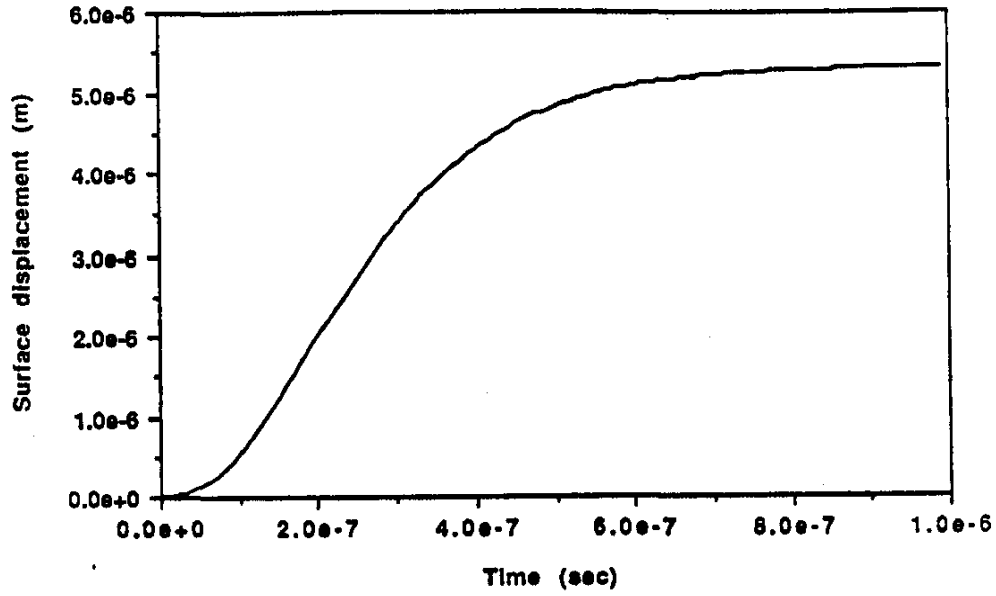

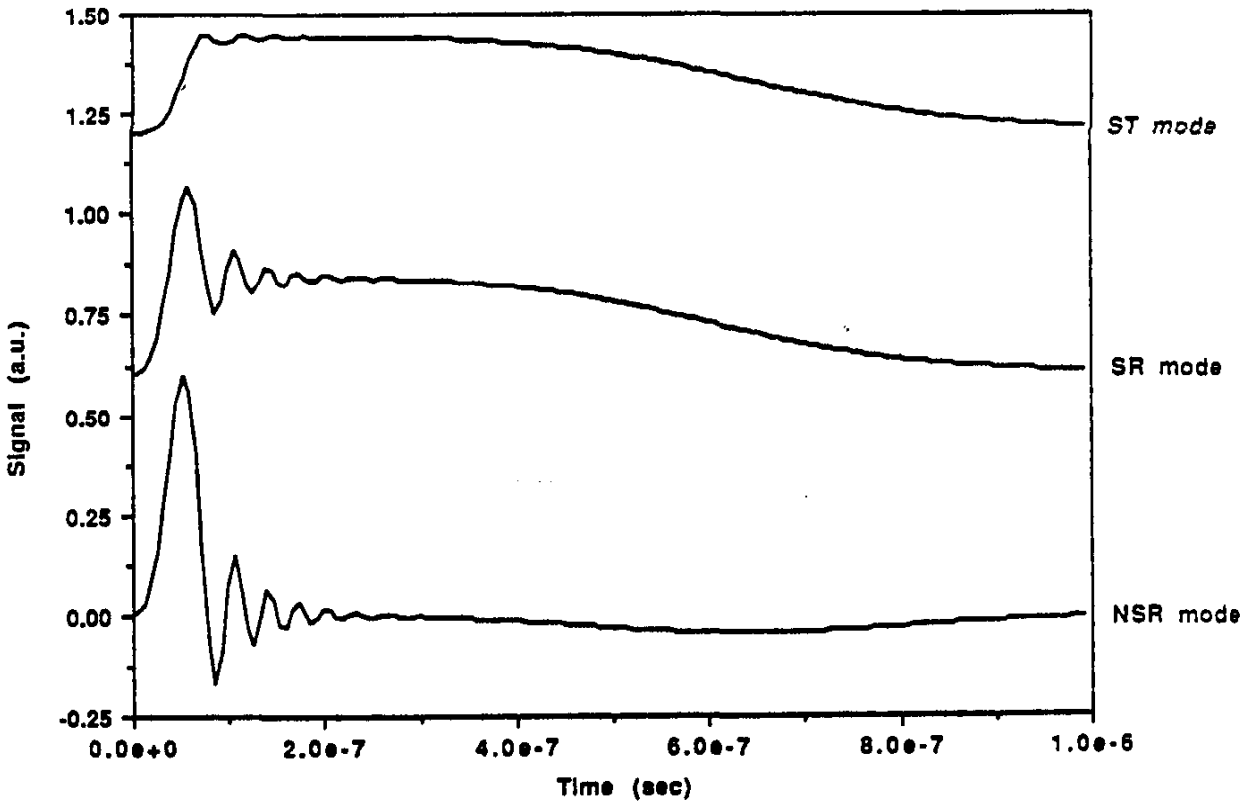

Figure 16 : Same as figure 15 but on an expanded time scale. The surface displacement (above) is plotted on the same time scale.

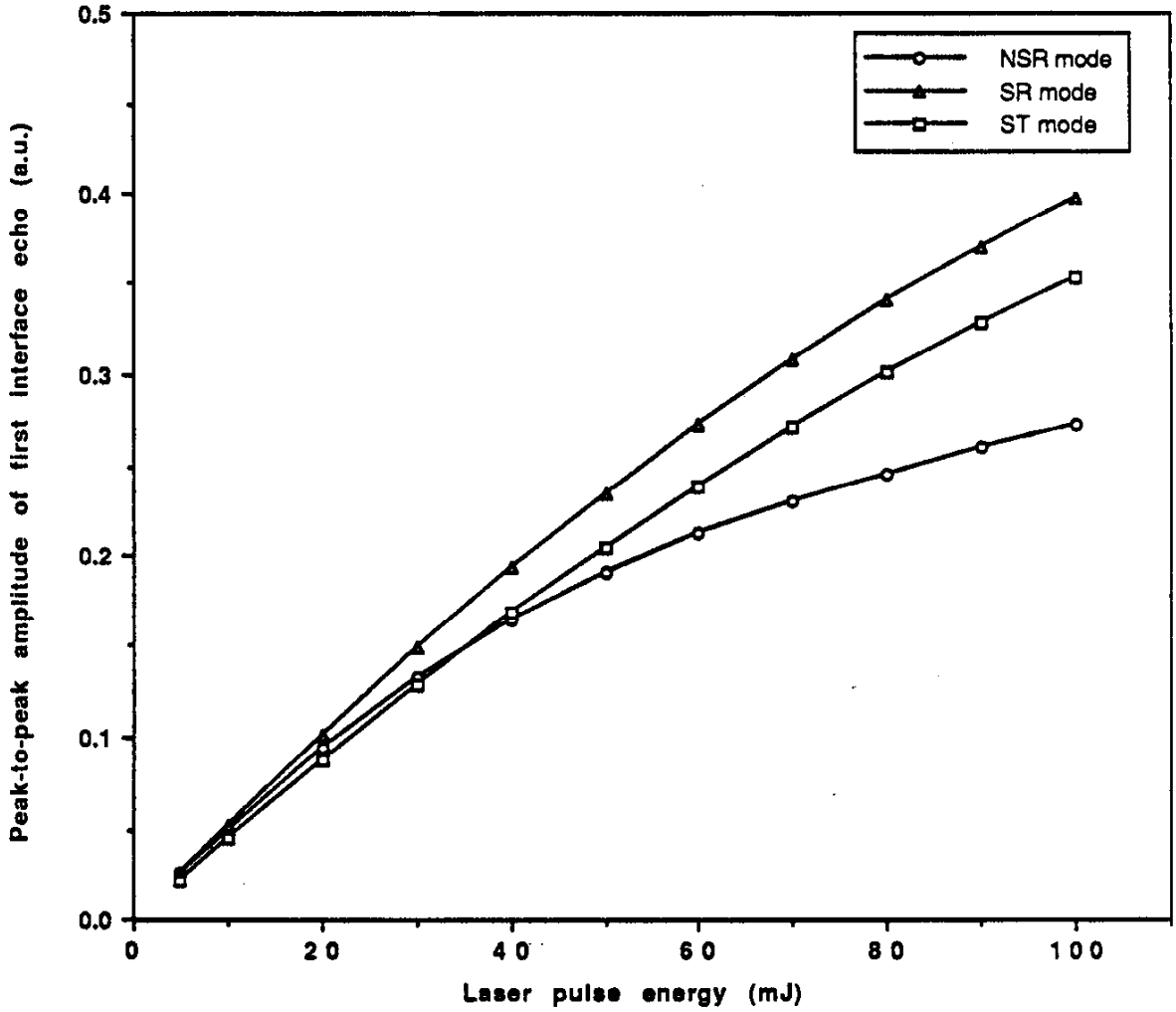

Figure 17 : Variation of the peak-to-peak amplitude of the first interface echo versus laser energy for three modes of operation.

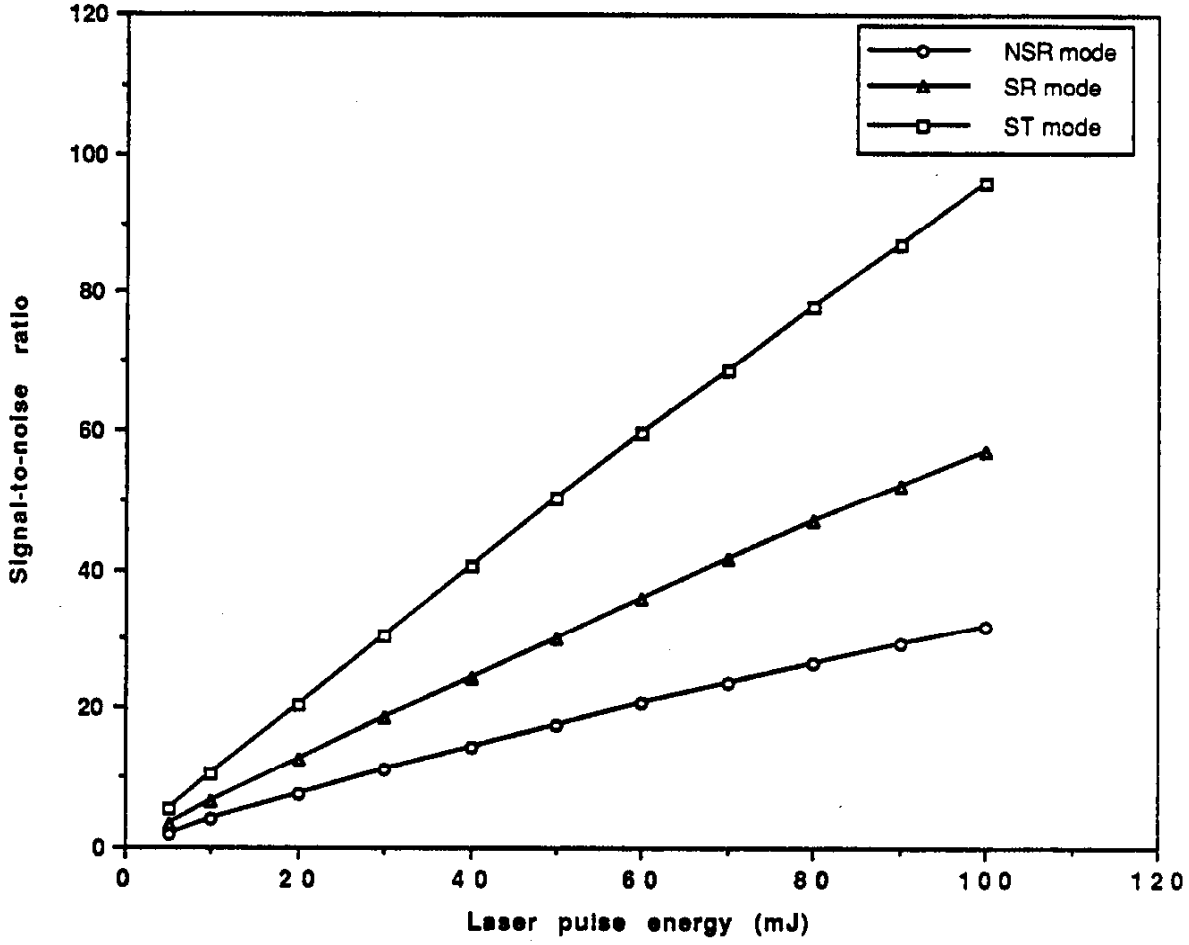

Figure 18 : Variation of the signal-to-noise ratio of the first interface echo versus laser energy for three modes of operation (finesse=10).

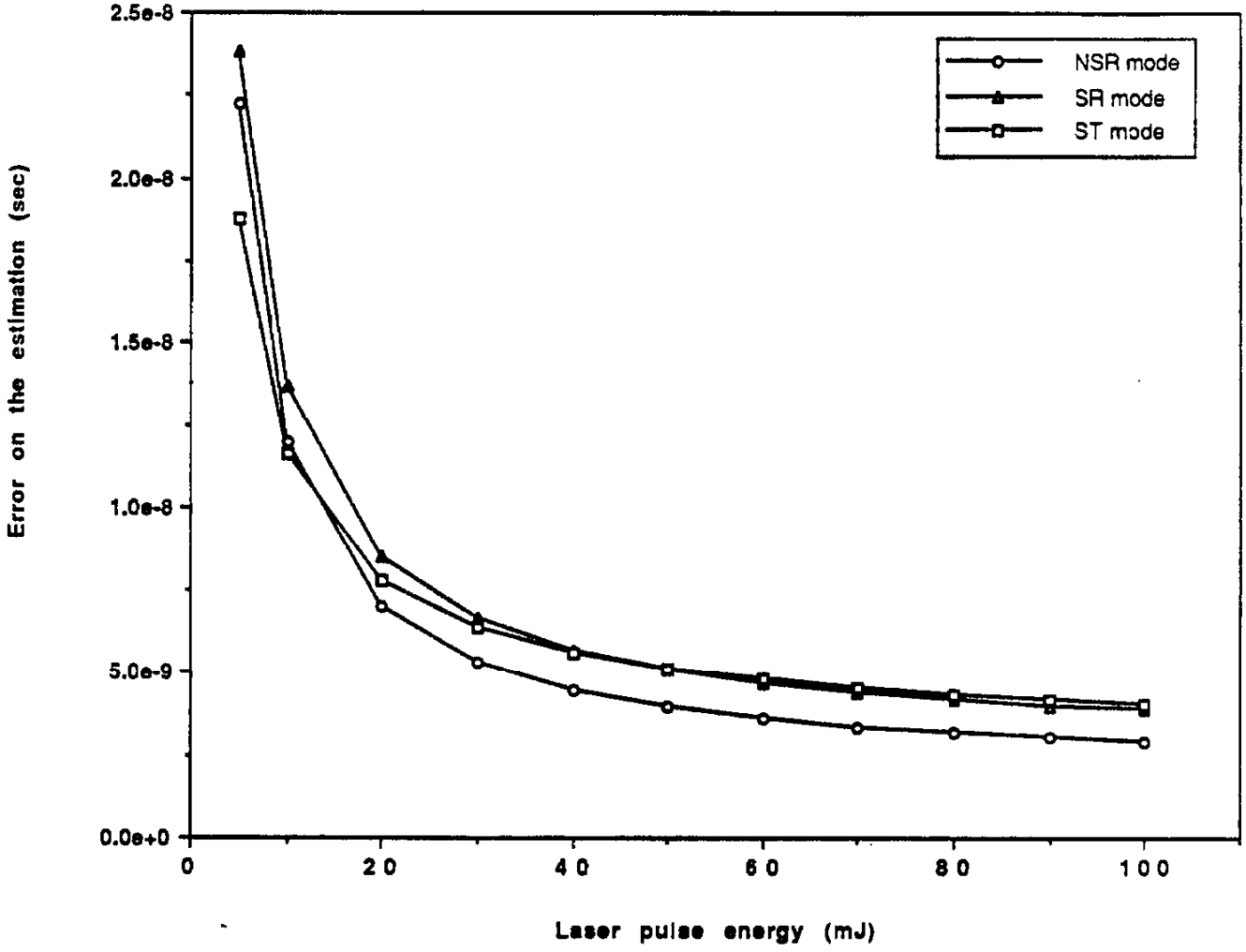

Figure 19 : Variation of the error of time delay determination versus laser energy for three modes of operation (finesse = 10).

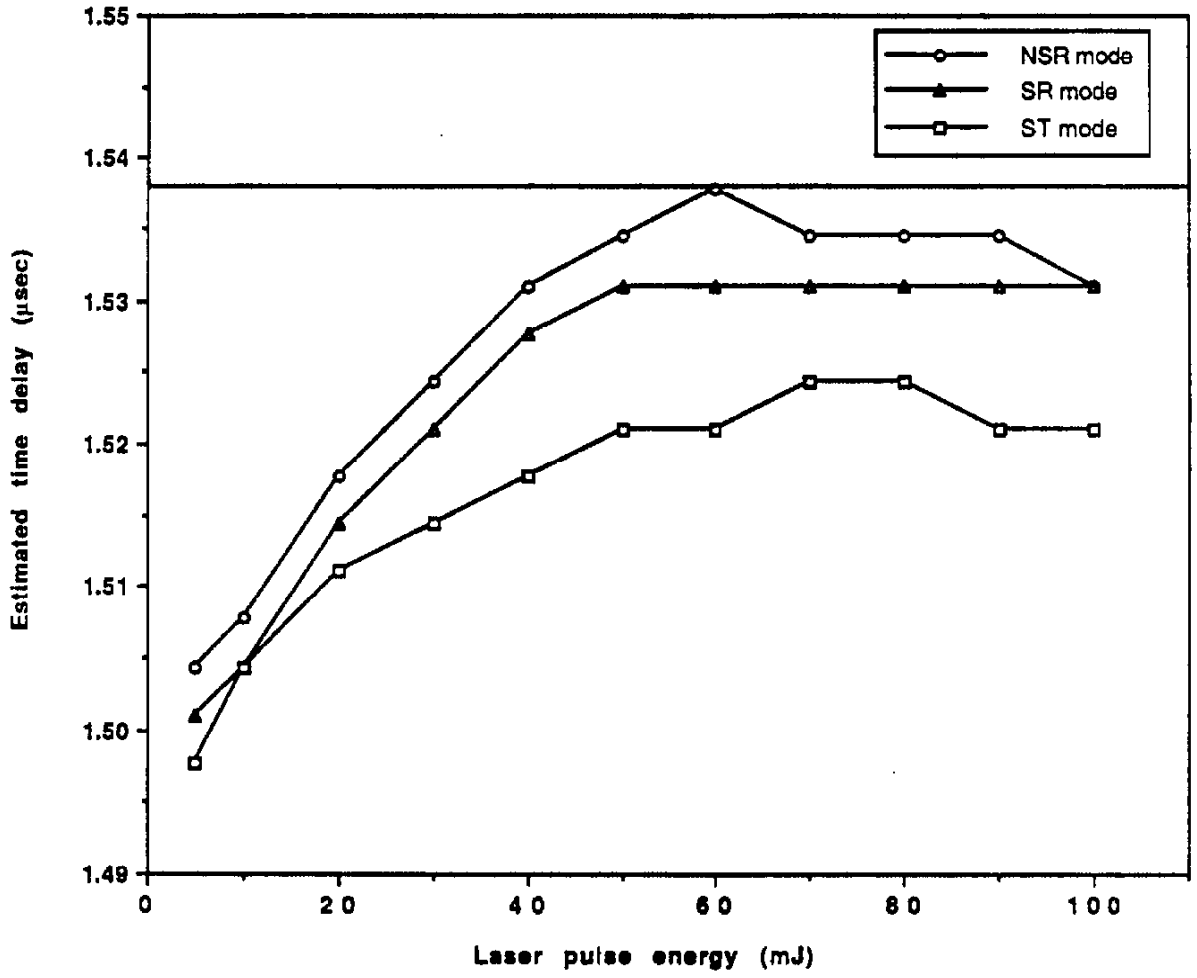

Figure 20 : Estimated delay versus laser pulse energy for three modes of operation (finesse=10). The horizontal line indicates the exact value.

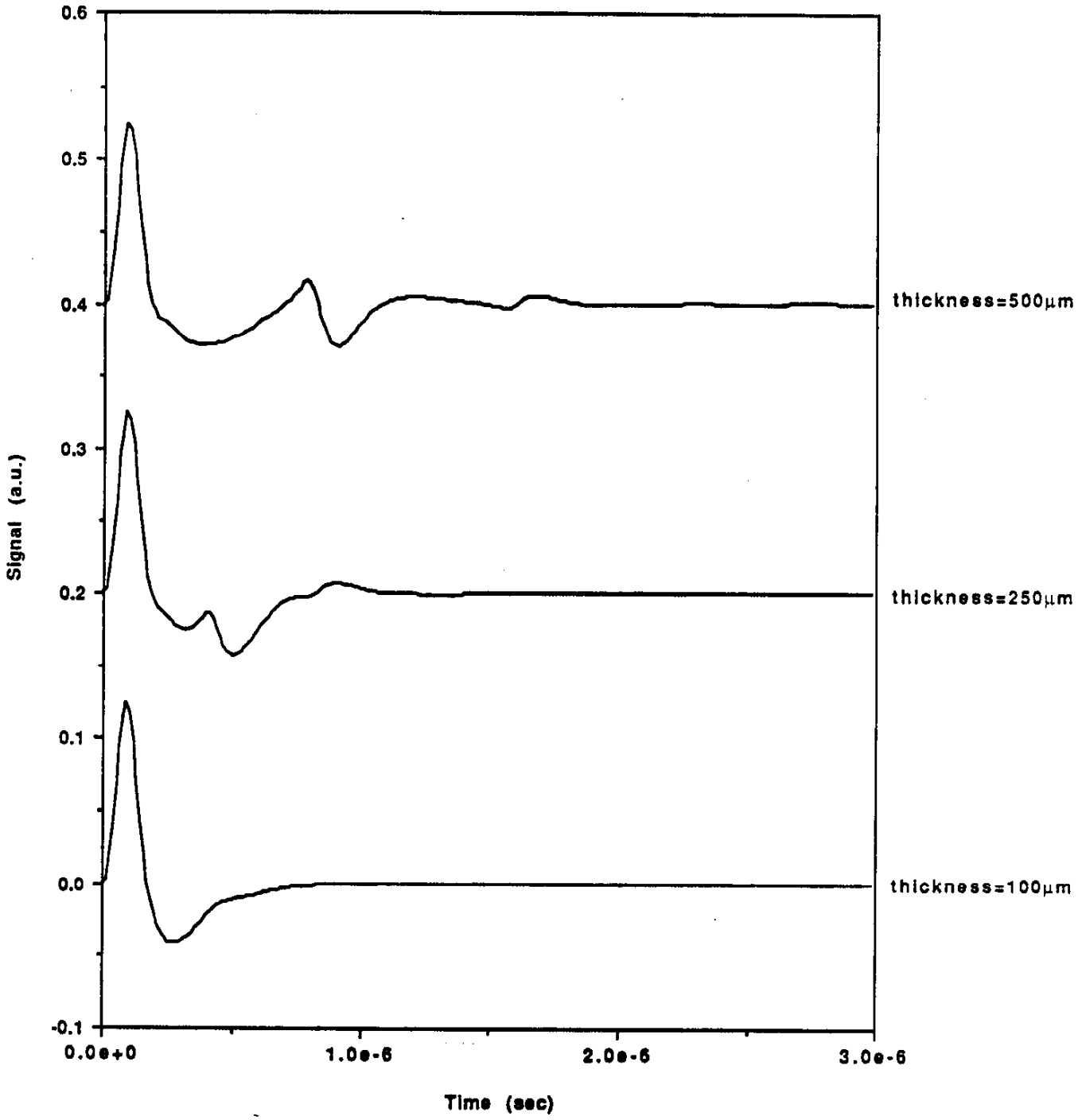

Figure 21 : Signal for several oil thicknesses, NSR mode, finesse=10, pulse energy=10 mJ.

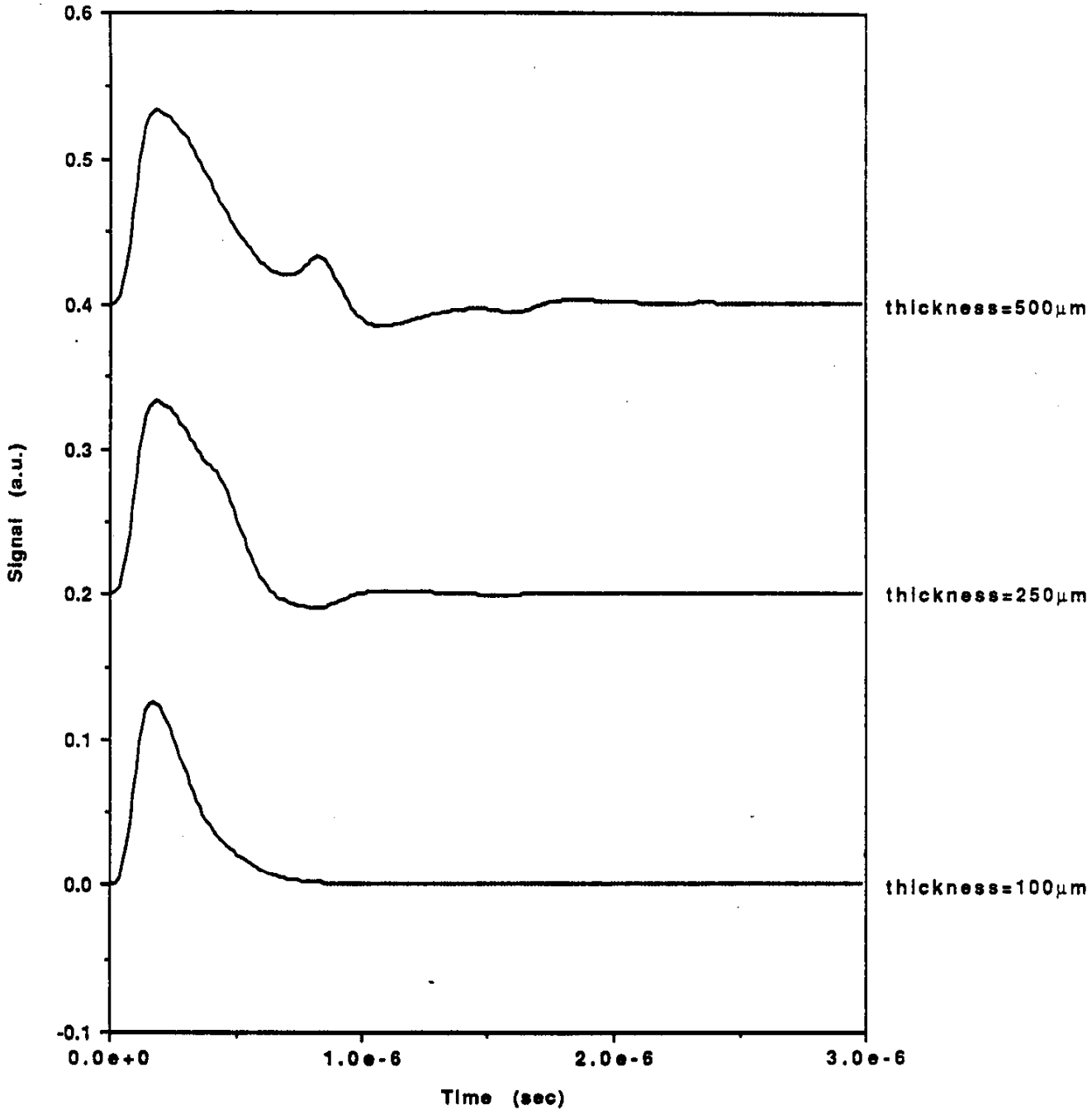

Figure 22 : Signal for severa oil thicknesses, ST mode, finesse=10, pulse energy=10 mJ.

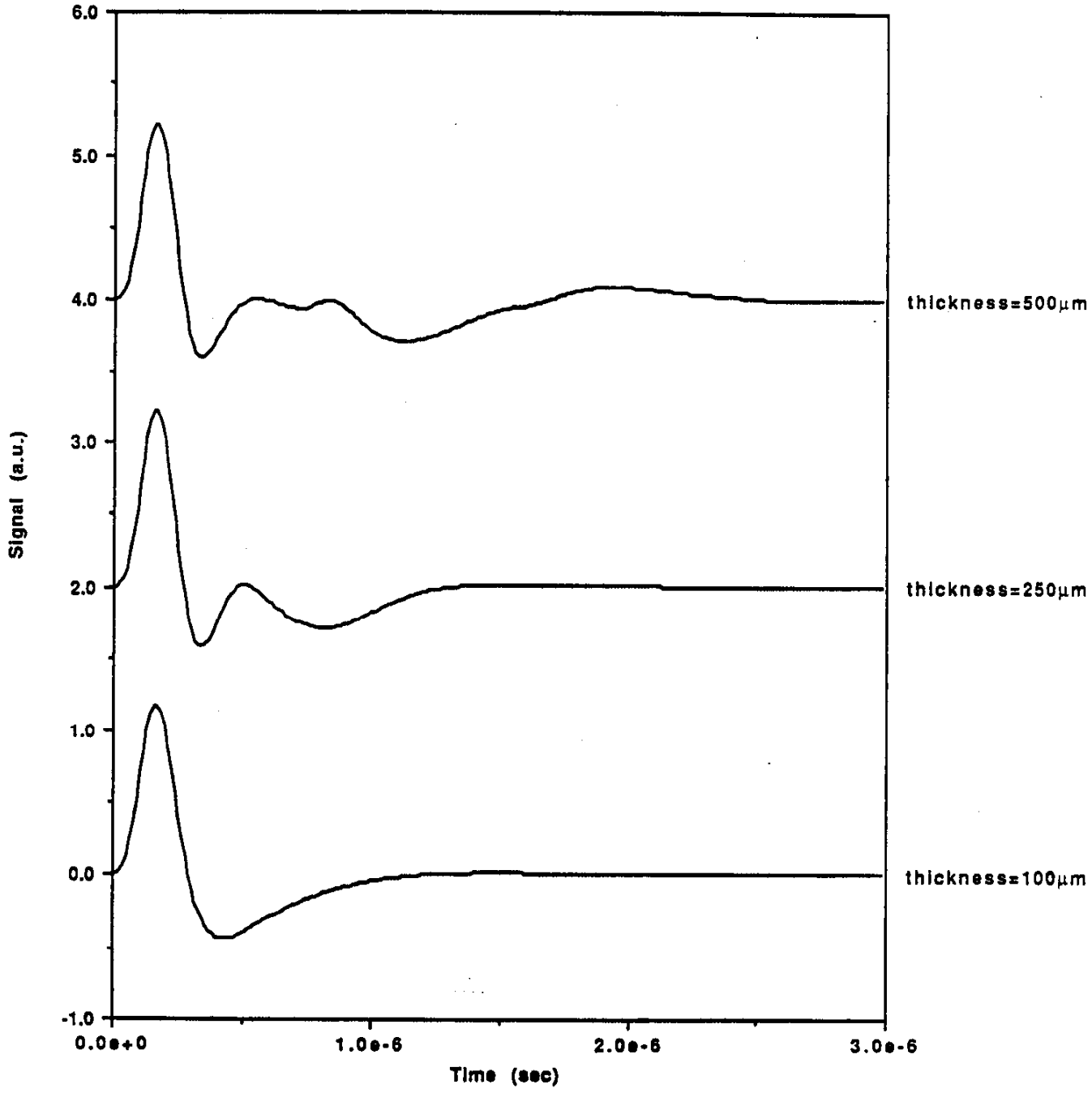

Figure 23 : Signal for several oil thicknesses, NSR mode, finesse=80, pulse energy=10 mJ.

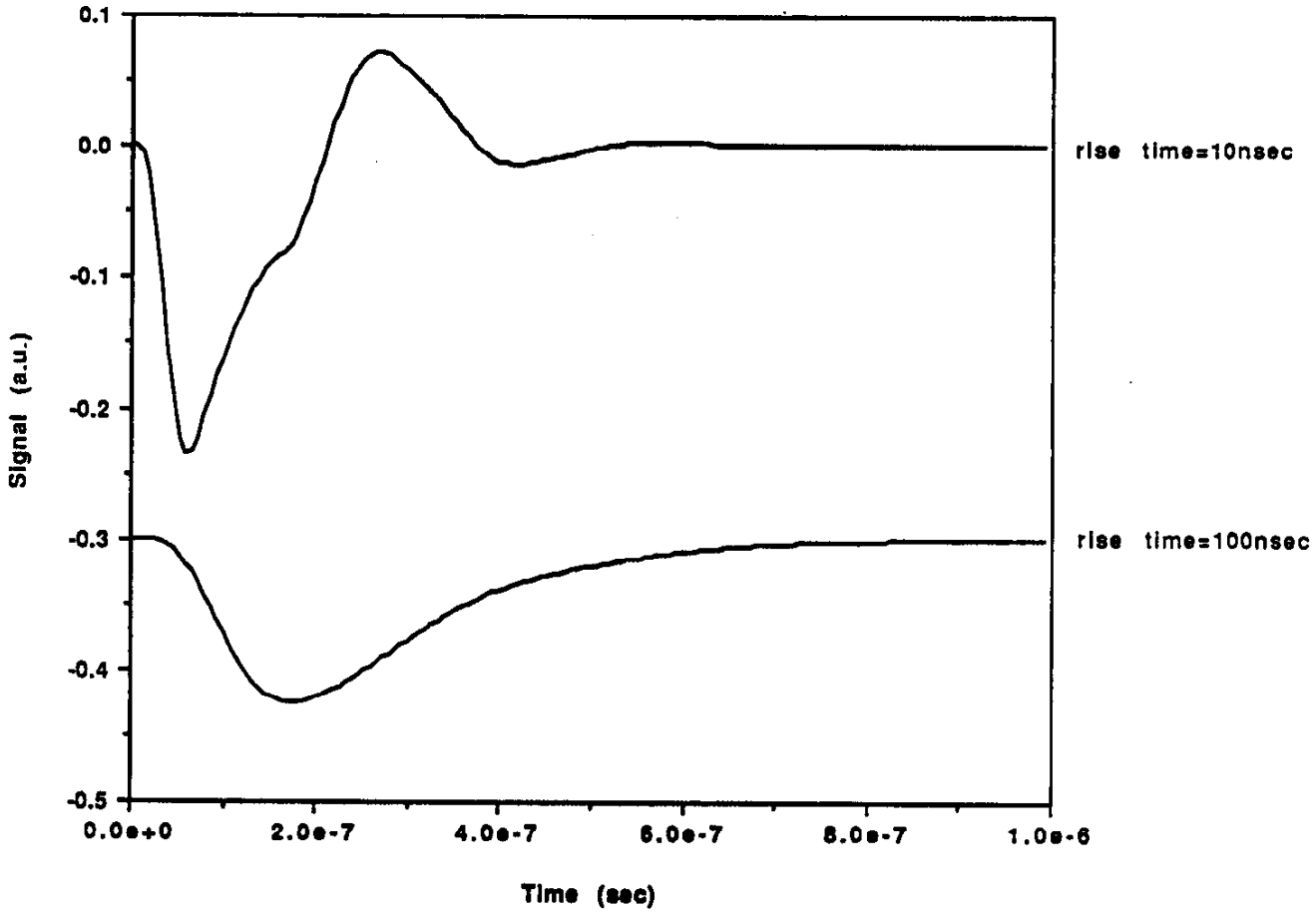

Figure 24 : Signals for two different laser pulse rise time (pulse shape $t/\tau \exp(-t/\tau)$), ST mode, finesse=10, pulse energy=10 mJ, thickness=100 μm.

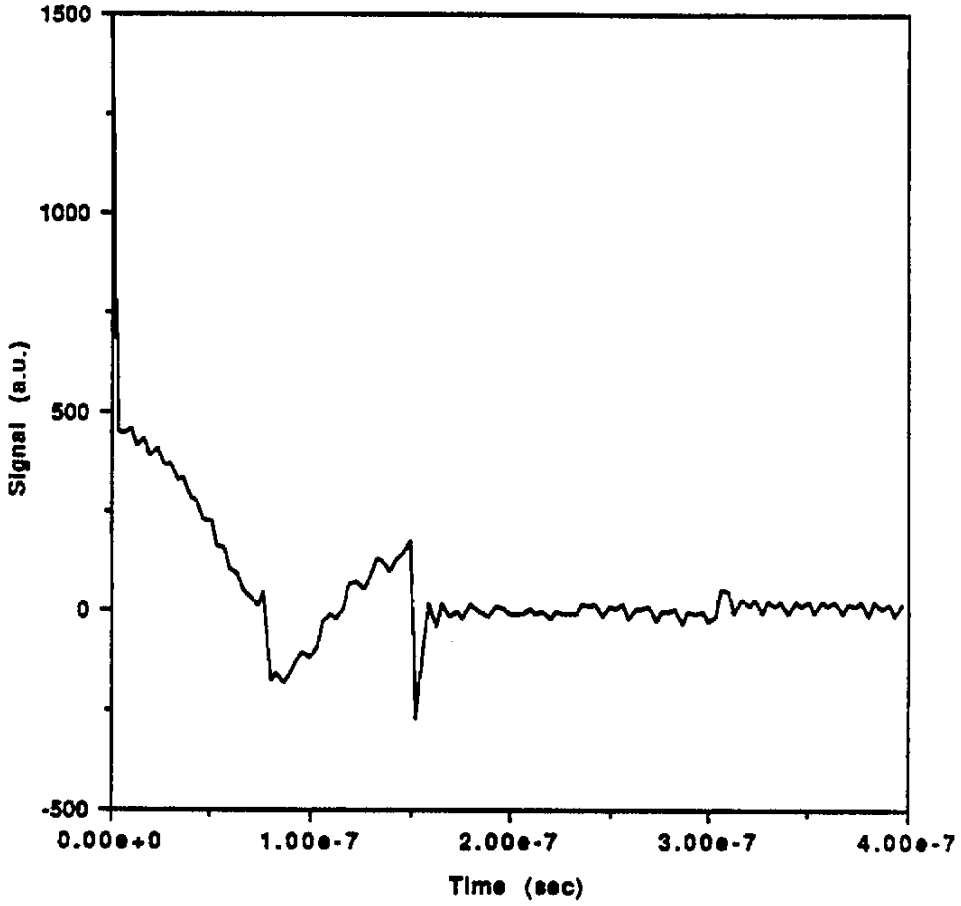

Figure 25 : Result of deconvolution by the signal generated on water only, oil layer thickness=100 ST mode, FP 1 m long, finesse=10, energy=10 mJ.

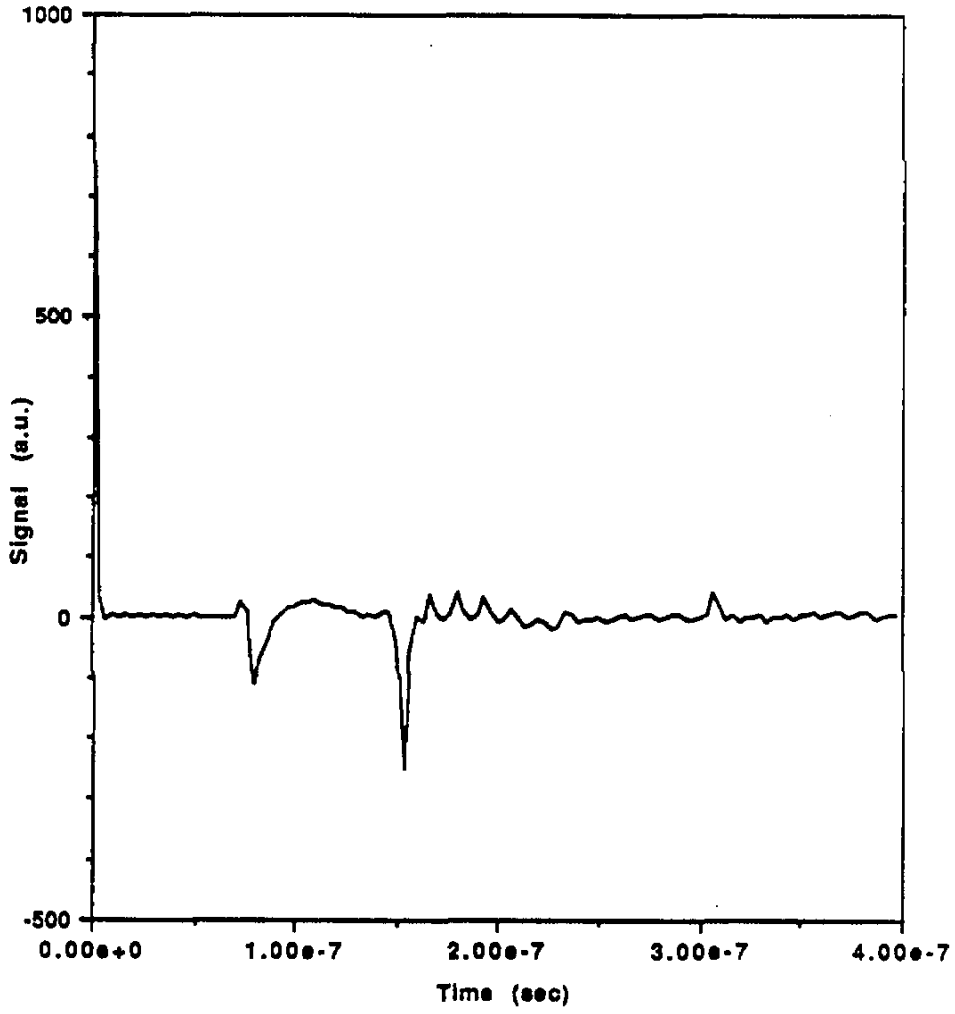

Figure 26 : Result of deconvolution by the signal generated on oil only, oil layer thickness=100 µm ST mode, FP 1 m long, finesse=10, laser energy=10 mJ.